J|A|C|S
A R T I C L E S

Intramolecular Hydroamination/Cyclization of Conjugated Aminodienes Catalyzed by Organolanthanide Complexes. Scope, Diastereo- and Enantioselectivity, and Reaction Mechanism

Sukwon Hong, Amber M. Kawaoka, and Tobin J. Marks*

Contribution from the Department of Chemistry, Northwestern University, 2145 Sheridan Road, Evanston, Illinois 60208-3113

Received May 21, 2003; E-mail: t-marks@northwestern.edu

Abstract: Organolanthanide complexes of the general type $Cp'_2LnCH(TMS)_2$ ($Cp' = \eta^5\text{-}Me_5C_5$; Ln = La, Sm, Y; TMS = SiMe$_3$) and $CGCSmN(TMS)_2$ (CGC = $Me_2Si(\eta^5\text{-}Me_4C_5)(^tBuN)$) serve as effective precatalysts for the rapid, regioselective, and highly diastereoselective intramolecular hydroamination/cyclization of primary and secondary amines tethered to conjugated dienes. The rates of aminodiene cyclizations are significantly more rapid than those of the corresponding aminoalkenes. This dienyl group rate enhancement as well as substituent group (R) effects on turnover frequencies is consistent with proposed transition state electronic demands. Kinetic and mechanistic data parallel monosubstituted aminoalkene hydroamination/ cyclization, with turnover-limiting C=C insertion into the Ln–N bond to presumably form an Ln-η^3 allyl intermediate, followed by rapid protonolysis of the resulting Ln–C linkage. The rate law is first-order in [catalyst] and zero-order in [aminodiene]. However, depending on the particular substrate and catalyst combination, deviations from zero-order kinetic behavior reflect competitive product inhibition or self-inhibition by substrate. Lanthanide ionic radius effects and ancillary ligation effects on turnover frequencies suggest a sterically more demanding Ln–N insertion step than in aminoalkene cyclohydroamination, while a substantially more negative $\Delta S^{\ddagger}$ implies a more highly organized transition state. Good to excellent diastereoselectivity is obtained in the synthesis of 2,5-*trans*-disubstituted pyrrolidines (80% de) and 2,6-*cis*-disubstituted piperidines (99% de). Formation of 2-(prop-1-enyl)piperidine using the chiral C_1-symmetric precatalyst (*S*)-Me$_2$Si(OHF)(CpR*)SmN(TMS)$_2$ (OHF = η^5-octahydrofluorenyl; Cp = η^5-C$_5$H$_3$; R* = (−)-menthyl) proceeds with up to 71% ee. The highly stereoselective feature of aminodiene cyclization is demonstrated by concise syntheses of naturally occurring alkaloids, (±)-pinidine and (+)-coniine from simple diene precursors.

Introduction

Catalytic N–H addition to C–C multiple bonds is a highly desirable, atom-economical transformation for the synthesis of organonitrogen molecules.[1] There has been a growing effort to develop efficient and selective catalysts for this challenging reaction.[2–5] Organolanthanides[6] are highly efficient catalysts for the inter-[7] and intramolecular hydroamination/cyclization of aminoalkenes,[8,9] aminoalkynes,[10] and aminoallenes,[11] reflecting the facile insertion of C–C unsaturation into lanthanide-ligand σ bonds (Scheme 1). Attractive features of organolanthanide catalysts include very high turnover frequencies, versatile reaction scope in terms of amines (both aliphatic and aromatic), substitution pattern and ring size,[12] and high stereoselectivity. Nevertheless, efficient cyclization of amine-tethered 1,2-disubstituted alkenes has remained elusive.[8a,8c,11b,13] Various α-alkyl
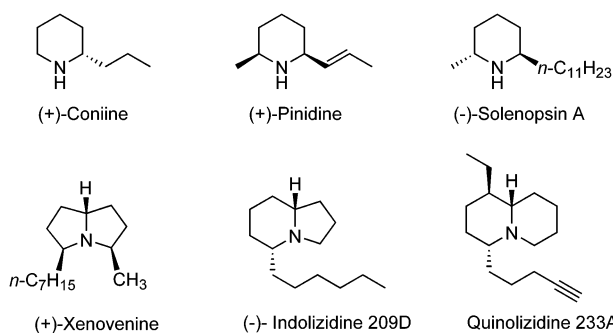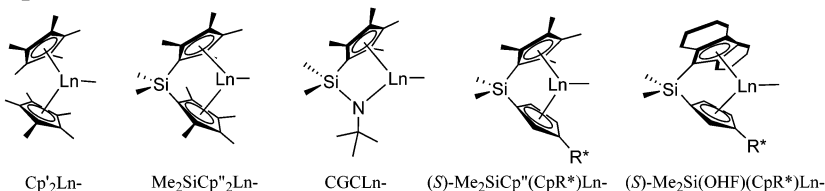
side chains can be found in naturally occurring alkaloids, and one can easily envision that stereoselective 1,2-disubstituted alkene hydroamination could be a very concise, elegant route to such substituted azacyles (Figure 1).[14] The proposed simplified mechanism for organolanthanide-catalyzed hydroamination

(1) For recent reviews of catalytic hydroamination, see: (a) Pohlki, F.; Doye, S. *Chem. Soc. Rev.* **2003**, *32*, 104−114. (b) Nobis, M.; Driessen-Hölscher, B. *Angew. Chem., Int. Ed.* **2001**, *40*, 3983−3985. (c) Brunet, J, J.; Neibecker, D. In *Catalytic Heterofunctionalization*; Togni, A., Grützmacher, H. Eds.; Wiley-VCH: Weinheim, 2001; pp 91−141. (d) Müller, T. E.; Beller, M. *Chem. Rev.* **1998**, *98*, 675−703.

(2) For recent examples of hydroamination catalyzed by late transition metals, see: (a) Fadini, L.; Togni, A. *Chem. Commun.* **2003**, 30−31. (b) Shimada, T.; Yamamoto, Y. *J. Am. Chem. Soc.* **2002**, *124*, 12670−12671. (c) Neff, V.; Müller, T. E.; Lercher, J. A. *Chem. Commun.* **2002**, 906−907. (d) Lutete, L. M.; Kadota, I.; Shibuya, A.; Yamamoto, Y. *Heterocycles* **2002**, *58*, 347−357. (e) Nettekoven, U.; Hartwig, J. F. *J. Am. Chem. Soc.* **2002**, *124*, 1166−1167. (f) Pawlas, J.; Nakao, Y.; Kawatsura, M.; Hartwig, J. F. *J. Am. Chem. Soc.* **2002**, *124*, 3669−3679. (g) Löber, O.; Kawatsura, M.; Hartwig, J. F. *J. Am. Chem. Soc.* **2001**, *123*, 4366−4367. (h) Minami, T.; Okamoto, H.; Ikeda, S.; Tanaka, R.; Ozawa, F.; Yoshifuji, M. *Angew. Chem., Int. Ed.* **2001**, *40*, 4501−4503. (i) Hartung, C. G.; Tillack, A.; Trauthwein, H.; Beller, M. *J. Org. Chem.* **2001**, *66*, 6339−6343. (j) Müller, T. E.; Berger, M.; Grosche, M.; Herdtweck, E.; Schmidtchen, F. P. *Organometallics* **2001**, *20*, 4384−4393. (k) Kawatsura, M.; Hartwig, J. F. *Organometallics* **2001**, *20*, 1960−1964. (l) Kawatsura, M.; Hartwig, J. F. *J. Am. Chem. Soc.* **2000**, *122*, 9546−9547. (m) Senn, H. M.; Blöchl, P. E.; Togni, A. *J. Am. Chem. Soc.* **2000**, *122*, 4098−4107. (n) Vasen, D.; Salzer, A.; Gerhards, F.; Gais, H.-J.; Stürmer, R.; Bieler, N. H.; Togni, A. *Organometallics* **2000**, *19*, 539−546. (o) Müller, T. E.; Grosche, M.; Herdtweck, E.; Pleier, A.-K.; Walter, E.; Yan, Y.-K. *Organometallics* **2000**, *19*, 170−183. (p) Burling, S.; Field, L. D.; Messerle, B. A. *Organometallics* **2000**, *19*, 87−90.

Scheme 1. Simplified Catalytic Cycle for the Organolanthanide-Mediated Hydroamination/Cyclization of Aminoalkenes, Aminoalkynes, and Aminoallenes
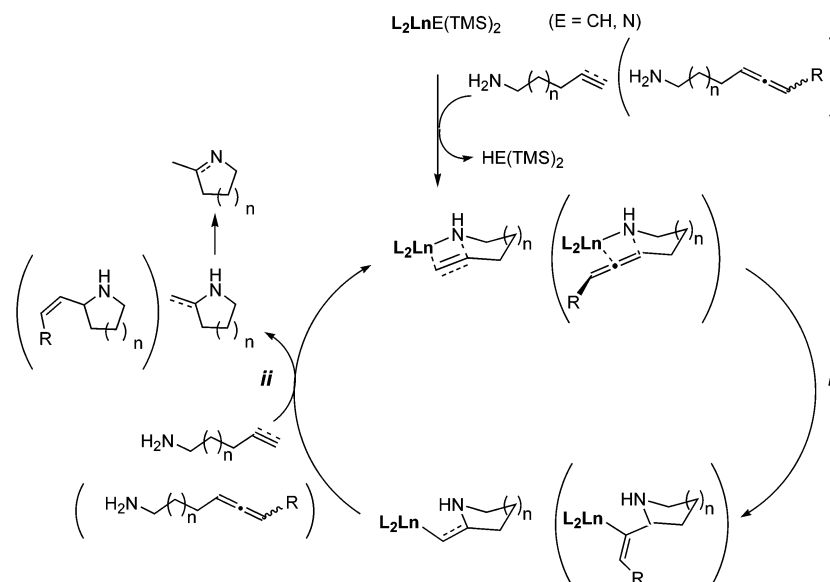
Estimated ΔH's (kcal/mol)

Unsaturation	Step i	Step ii
Aminoalkene	0	-13
Aminoallene	-29	0
Aminoalkyne	-35	0

L_2Ln- =

Cp'$_2$Ln-   Me$_2$SiCp''$_2$Ln-   CGCLn-   (*S*)-Me$_2$SiCp''(CpR*)Ln-   (*S*)-Me$_2$Si(OHF)(CpR*)Ln-

(+)-Coniine   (+)-Pinidine   (-)-Solenopsin A

(+)-Xenovenine   (-)- Indolizidine 209D   Quinolizidine 233A

Figure 1. Examples of naturally occurring alkaloids containing various α-side chains.

involves a turnover-limiting, sterically sensitive olefin insertion step (Scheme 1, step i) via a four-centered transition state, followed by rapid protonlysis of the resulting Ln–C bond (Scheme 1, step ii).[8j,10c,11b] The inherent limitation in 1,2-disubstituted alkene insertion is reasonably attributed to severe nonbonded steric repulsions[8c,i] and a possible charge separation imbalance in the relatively well-characterized transition state (**A**).[8j] Previously, we addressed this issue via two different
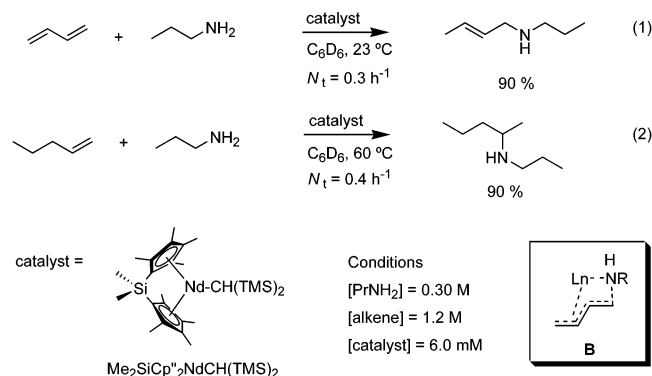

A
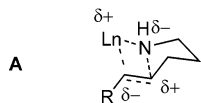
strategies. First, new aminoallene substrates[11] were developed. In contrast to aminoalkenes, aminoallene cyclization tolerates further substitution at the terminal position of allenyl groups, as previously observed with aminoalkynes.[10c] This methodology was successfully applied to the concise synthesis of the pyrrolizidine alkaloid, (+)-xenovenine.[11a] However, the intrinsic chirality of an allenyl group[15] and the rather sluggish rate of a

(3) For recent examples of hydroamination catalyzed by early transition metals, see: (a) Shi, Y.; Hall, C.; Ciszewski, J. T.; Cao, C.; Odom, A. L. *Chem. Commun.* **2003**, 586–587. (b) Tillack, A.; Castro, I. G.; Hartung, C. G.; Beller, M. *Angew. Chem., Int. Ed.* **2002**, *41*, 2541–2543. (c) Cao, C.; Shi, Y.; Odom, A. L. *Org. Lett.* **2002**, *4*, 2853–2856. (d) Ong, T.-G.; Yap, G. P. A.; Richeson, D. S. *Organometallics* **2002**, *21*, 2839–2841. (e) Ackermann, L.; Bergman, R. G. *Org. Lett.* **2002**, *4*, 1475–1478. (f) Heutling, A.; Doye, S. *J. Org. Chem.* **2002**, *67*, 1961–1964. (g) Straub, B. F.; Bergman, R. G. *Angew. Chem., Int. Ed.* **2001**, *40*, 4632–4635. (h) Cao, C.; Ciszewski, J. T.; Odom, A. L. *Organometallics* **2001**, *20*, 5011–5013. (i) Johnson, J. S.; Bergman, R. G. *J. Am. Chem. Soc.* **2001**, *123*, 2923–2924. (j) Shi, Y.; Ciszewski, J. T.; Odom, A. L. *Organometallics* **2001**, *20*, 3967–3969. (k) Pohlki, F.; Doye, S. *Angew. Chem., Int. Ed.* **2001**, *40*, 2305–2308. (l) Haak, E.; Siebeneicher, H.; Doye, S. *Org. Lett.* **2000**, *2*, 1935–1937.

(4) For recent examples of hydroamination catalyzed by actinide metals, see: (a) Wang, J.; Dash, A. K.; Kapon, M.; Berthet, J.-C.; Ephritikhine, M.; Eisen, M. S. *Chem.—Eur. J.* **2002**, *8*, 5384–5396. (b) Straub, T.; Haskel, A.; Neyroud, T. G.; Kapon, M.; Botoshansky, M.; Eisen, M. S. *Organometallics* **2001**, *20*, 5017–5035. (c) Haskel, A.; Straub, T.; Eisen, M. S. *Organometallics* **1996**, *15*, 3773–3775.

(5) For recent examples of base-catalyzed hydroaminations, see: (a) Trost, B. M.; Tang, W. *J. Am. Chem. Soc.* **2002**, *124*, 14542–14543. (b) Hartung, C. G.; Breindl, C.; Tillack, A.; Beller, M. *Tetrahedron* **2000**, *56*, 5157–5162. For recent examples of acid-catalyzed hydroaminations, see: (c) Miura, K.; Hosomi, A. *Synlett* **2003**, 143–155. (d) Schlummer, B.; Hartwig, J. F. *Org. Lett.* **2002**, *4*, 1471–1474.
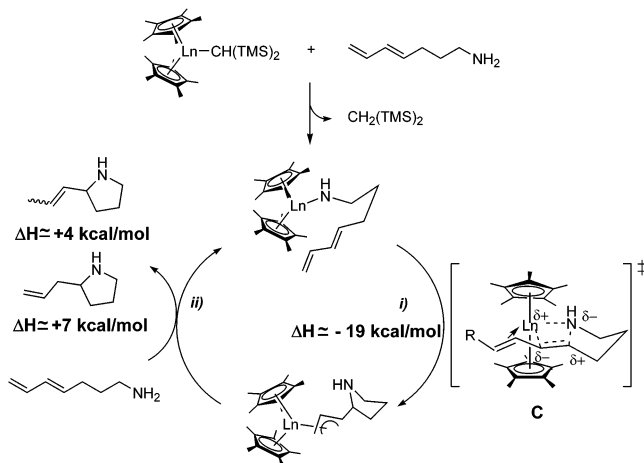
six-membered ring formation render aminoallenes less attractive for enantioselective hydroamination/cyclization studies. Second, we also demonstrated that hydroamination/cyclization of amine-tethered 1,2-disubstituted alkenes proceeds at elevated reaction temperatures (120–130 °C) with catalysts of large metal ionic radii/high coordinative unsaturation.[8a,c] However, alkyl substitution on the tether region appears to be necessary for reasonable turnover frequencies.

Alternatively, from preliminary *intermolecular* organolanthanide-mediated diene hydroamination results,[7b] we envisioned conjugated diene substrates as attractive precursors for the synthesis of azacyclic targets. At comparable concentrations, intermolecular diene hydroamination is significantly more rapid than alkene hydroamination (eq 1 versus eq 2), and lanthanide η^3-crotyl intermediate **B** was proposed based upon literature precedent.[16] In addition, note that one of the recent advances

in late transition metal-mediated hydroamination systems have been made by utilizing conjugated alkenes such as styrenes[2e,l] and 1,3-dienes[2f,g] for Pd-catalyzed intermolecular hydroamination.

(6) For recent organolanthanide reviews, see: (a) Aspinall, H. C. *Chem. Rev.* **2002**, 1807–1850. (b) Edelmann, F. T.; Freckmann, D. M. M.; Schumann, H. *Chem. Rev.* **2002**, 1851–1896. (c) Arndt, S.; Okuda, J. *Chem. Rev.* **2002**, 1953–1976. (d) Molander, G. A.; Romero, J. A. C. *Chem. Rev.* **2002**, 2161–2185. (e) *Topics in Organometallic Chemistry*; Kobayashi, S. Ed.; Springer: Berlin, 1999; Vol 2. (f) Edelmann, F. T. *Top. Curr. Chem.* **1996**, *179*, 247–276. (g) Schumann, H.; Meese-Marktscheffel, J. A.; Esser, L. *Chem. Rev.* **1995**, *95*, 865–986. (h) Schaverien, C. J. *Adv. Organomet. Chem.* **1994**, *36*, 283–362.
(7) (a) Ryu, J.-S.; Li, G. Y.; Marks, T. J. *J. Am Chem. Soc.* **2003**, *125*, 12584–12605. (b) Li, Y.; Marks, T. J. *Organometallics* **1996**, *15*, 3770–3772.
(8) (a) Ryu, J.-S.; McDonald, F. E.; Marks, T. J. *J. Org. Chem.*, in press. (b) Kim, Y. K.; Livinghouse, T. *Angew. Chem., Int. Ed.* **2002**, *41*, 3645–3647. (c) Ryu, J.-S.; Marks, T. J.; McDonald, F. E. *Org. Lett.* **2001**, *3*, 3091–3094. (d) Molander, G. A.; Dowdy, E. D.; Pack, S. K. *J. Org. Chem.* **2001**, *66*, 4344–4347. (e) Kim, Y. K.; Livinghouse, T.; Bercaw, J. E. *Tetrahedron Lett.* **2001**, *42*, 2933–2935. (f) Molander, G. A.; Dowdy, E. D. *J. Org. Chem.* **1999**, *64*, 6515–6517. (g) Tian, S.; Arredondo, V. M.; Stern, C. L.; Marks, T. J. *Organometallics* **1999**, *18*, 2568–2570. (h) Gilbert, A. T.; Davis, B. L.; Emge, T. J.; Broene, R. D. *Organometallics* **1999**, *18*, 2125–2132. (i) Molander, G. A.; Dowdy, E. D. *J. Org. Chem.* **1998**, *63*, 8983–8988. (j) Gagné, M. R.; Stern, C. L.; Marks, T. J. *J. Am Chem. Soc.* **1992**, *114*, 275–294. (k) Gagné, M. R.; Nolan, S. P.; Marks, T. J. *Organometallics* **1990**, *9*, 1716–1718. (l) Gagné, M. R.; Marks, T. J. *J. Am. Chem. Soc.* **1989**, *111*, 4108–4109.
(9) (a) Douglass, M. R.; Ogasawara, M.; Hong, S.; Metz, M. V.; Marks, T. J. *Organometallics* **2002**, *21*, 283–292. (b) Giardello, M. A.; Conticello, V. P.; Brard, L.; Gagné, M. R.; Marks, T. J. *J. Am. Chem. Soc.* **1994**, *116*, 10241–10254. (c) Giardello, M. A.; Conticello, V. P.; Brard, L.; Sabat, M.; Rheingold, A. L.; Stern, C. L.; Marks, T. J. *J. Am. Chem. Soc.* **1994**, *116*, 10212–10240. (d) Gagné, M. R.; Brard, L.; Conticello, V. P.; Giardello, M. A.; Stern, C. L.; Marks, T. J. *Organometallics* **1992**, *11*, 2003–2005.
(10) (a) Li, Y.; Marks, T. J. *J. Am. Chem. Soc.* **1998**, *120*, 1757–1771. (b) Bürgstein, M. R.; Berberich, H.; Roesky, P. W. *Organometallics* **1998**, *17*, 1452–1454. (c) Li, Y.; Marks, T. J. *J. Am. Chem. Soc.* **1996**, *118*, 9295–9306. (d) Li, Y.; Marks, T. J. *J. Am. Chem. Soc.* **1996**, *118*, 707–708. (e) Li, Y.; Fu, P.-F.; Marks, T. J. *Organometallics* **1994**, *13*, 439–440.

Scheme 2. Proposed Catalytic Cycle for the Organolanthanide-Mediated Hydroamination of Conjugated Aminodienes

Thermodynamic considerations[17] for the prospective organolanthanide-mediated hydroamination of conjugated dienes predict that insertion (Scheme 2, step i) is significantly more exothermic (~ -19 kcal/mol) than for terminal alkenes (~ 0 kcal/mol), whereas the subsequent protonolysis (Scheme 2, step ii) is slightly endothermic ($\sim +4$ or $+7$ kcal/mol), unlike the exothermic protonolysis for the terminal alkene cycle (~ -13 kcal/mol).[18] In our previous communication, we reported that this transformation proceeds smoothly for a range of substrates with good rates and high diastereo- and enantioselectivity.[19] Attractive features of aminodiene cyclizations are seen to include significant rate enhancements versus terminal alkene substrates and high stereoselectivities as demonstrated in the concise syntheses of the natural products, (±)-pinidine and (+)-coniine. Herein we present comprehensive kinetic/mechanistic studies on aminodiene hydroamination and discuss further optimizing efforts on diastereo- and enantioselectivity. In this full account, reaction scope, various factors affecting reaction rates and stereoselectivity, and kinetic observations are discussed/

(11) (a) Arredondo, V. M.; Tian, S.; McDonald, F. E.; Marks, T. J. *J. Am. Chem. Soc.* **1999**, *121*, 3633–3639. (b) Arredondo, V. M.; McDonald, F. E.; Marks, T. J. *Organometallics* **1999**, *18*, 1949–1960. (c) Arredondo, V. M.; McDonald, F. E.; Marks, T. J. *J. Am. Chem. Soc.* **1998**, *120*, 4871–4872.
(12) For a discussion of functional group tolerance in organolanthanide catalysis, see: (a) Molander, G. A. *Chemtracts: Org. Chem.* **1998**, *11*, 237–263. (b) Reference 7a.
(13) Hydroamination of 1,1-disubstituted alkenes has been reported by Molander;[8i] however, hydroamination of 1,2-disubstituted alkenes with the same catalyst was not successful.
(14) For example, the scope of enantioselective intramolecular hydroamination/cyclization by chiral organolanthanide was previously limited to mono-substituted alkenes, affording only methyl substituted chiral azacycles.
(15) AgBF₄-mediated cyclization of a chiral aminoallene to afford a 2-substituted piperidine in 78% ee: Lathbury, D.; Gallagher, T. *J. Chem. Soc., Chem. Commun.* **1986**, 114–115.
(16) For discussions of η^3-lanthanide allyls, see: (a) Evans, W. J.; Ulibarri, T. A.; Ziller, J. W. *J. Am. Chem. Soc.* **1990**, *112*, 2314–2324. (b) Bunel, E.; Burger, B. J.; Bercaw, J. E. *J. Am. Chem. Soc.* **1988**, *110*, 976–978 (c) Jeske, G.; Lauke, H.; Mauermann, H.; Swepston, P. N.; Schumann, H.; Marks, T. J. *J. Am. Chem. Soc.* **1985**, *107*, 8091–8103.
(17) Bond enthalpy data: (a) Nolan, S. P.; Stern, D.; Marks, T. J. *J. Am. Chem. Soc.* **1989**, *111*, 7844–7853. (b) McMillen, D. F.; Golden, D. M. *Annu. Rev. Phys. Chem.* **1982**, *33*, 493–532.
(18) (a) The ΔH for CH₃NH₂ addition to 1,3-butadiene (to yield (CH₂=CHCH₂-CH₂NH₂)) is estimated to be -12 kcal/mol (±0.6). (b) Pedley, J. B.; Naylor, R. D.; Kirby, S. P. *Thermochemical Data for Organic Compounds*, 2nd ed.; Chapman and Hall: London, 1986. (c) Nolan, S. P.; Stern, D.; Marks, T. J. *J. Am. Chem. Soc.* **1989**, *111*, 7844–7853.
(19) (a) Hong, S.; Marks, T. J. *J. Am. Chem. Soc.* **2002**, *124*, 7886–7887. (b) Hong, S.; Marks, T. J. *Abstract of Papers*; communicated in part at the 221st National ACS Meeting, San Diego, CA; April 2001; American Chemical Society: Washington, DC, 2001; abstract INOR 613.

interpreted in detail and compared/contrasted with previously identified hydroamination patterns.

Experimental Section

Materials and Methods. All manipulations of air-sensitive materials were carried out with rigorous exclusion of oxygen and moisture in flame- or oven-dried Schlenk-type glassware on a dual-manifold Schlenk line, or interfaced to a high-vacuum line (10^{-6} Torr), or in a nitrogen-filled Vacuum Atmospheres glovebox with a high capacity recirculator (<1 ppm of O_2). Argon (Matheson, prepurified) was purified by passage through a MnO oxygen-removal column and a Davison 4A molecular sieve column. Pentane and toluene were dried using activated alumina columns according to the method described by Grubbs[20] and were additionally vacuum-transferred from Na/K alloy immediately before use if employed for catalyst synthesis or catalytic reactions. Ether, THF, and dichloromethane were distilled before use from appropriate drying agents (sodium benzophenone ketyl, Na/K alloy, CaH_2, respectively) under nitrogen. Chloroform-d was purchased from Cambridge Isotope Laboratories. Benzene-d_6, toluene-d_8, and cyclohexane-d_{12} (Cambridge Laboratories; all 99+ atom % D) used for NMR reactions and kinetic measurements were stored in vacuo over Na/K alloy in resealable bulbs and were vacuum transferred immediately prior to use. All organic starting materials were purchased from Aldrich Chemical Co. or Lancaster Synthesis Inc. and were used without further purification unless otherwise stated. All substrates were dried twice as solutions in benzene-d_6 or toluene-d_8 over freshly activated Davison 4A molecular sieves and were degassed by freeze–pump–thaw methods. The substrates were then stored in vacuum-tight storage flasks. The organolanthanide precatalysts $Cp'_2LnCH(TMS)_2$ (Ln = La, Sm, Y; $Cp' = \eta^5\text{-Me}_5C_5$)[16c] and $CGCLnN(TMS)_2$ (CGC = Me_2-$Si(Me_4C_5)(^tBuN)$; Ln = Sm, Y)[8g] were prepared according to published procedures. We thank Dr. Masamichi Ogasawara for a sample of (*S*)-$Me_2Si(OHF)(CpR^*)SmN(TMS)_2$ (OHF = η^5-octahydrofluorenyl; Cp = η^5-C_5H_3; $R^* = (-)$-menthyl).[9a]

Physical and Analytical Measurements. NMR spectra were recorded on either a Varian Gemini 300 (FT, 300 MHz, ^{1}H; 75 MHz, ^{13}C), Unity- or Mercury-400 (FT, 400 MHz, ^{1}H; 100 MHz, ^{13}C), or Inova-500 (FT, 500 MHz, ^{1}H; 125 MHz, ^{13}C) instrument. Chemical shifts (δ) for ^{1}H and ^{13}C are referenced to internal solvent resonances and reported relative to SiMe$_4$. NMR experiments on air-sensitive samples were conducted in Teflon valve-sealed tubes (J. Young). HRMS studies were conducted on a VG 70-250 SE instrument with 70 eV electron impact ionization or chemical ionization using CH_4 as a reagent gas. Elemental analyses were performed by Midwest Microlabs, Indianapolis, IN. GC–MS analyses were performed using an HP6890 instrument equipped with an HP 5972 detector, an HP-5MS (5% Phenyl Methyl Siloxane, 30 m × 250 μm × 0.25 μm) capillary column, and Chemstation software. HPLC analyses were performed using a Waters Breeze system consisting of a model 1525 binary pump, model 77251 manual injector, and model 2487 dual λ UV/vis detector. Optical rotations were measured using an Optical Activity AA-100 polarimeter. IR spectra were recorded using a Biorad FT S60 FTIR instrument.

Typical NMR-Scale Catalytic Reactions. In the glovebox, the organolanthanide precatalyst (3–8 mg) was weighed into a 5-mm NMR tube equipped with a Teflon valve (J-Young), and C_6D_6 (0.5 mL) was added. The tube was then removed from the glovebox and attached to the high vacuum line. On the vacuum line, the tube was evacuated while the benzene solution was frozen at $-78°$ C. The substrate (ca. 1 M in C_6D_6, 0.15–0.3 mL, 10–40-fold molar excess) was added via syringe under an Ar flush. The tube was next evacuated and backfilled with Ar 3 times while frozen at -78 °C. The tube was then sealed, thawed, and brought to the desired temperature, and the ensuing reaction

was monitored by ^{1}H NMR. After the reaction was complete, the reaction mixture was freeze–thaw degassed and the volatiles were vacuum transferred into a separate NMR tube. The solvent was removed on a rotary evaporator at 0 °C to give the product. Alternatively, for nonvolatile products, filtration of the reaction mixture through a short pad of silica gel removes the catalyst. The silica gel was rinsed with Et_2O (5 mL); the fractions were combined and evaporated under reduced pressure to afford the product.

Low-Temperature NMR-Scale Catalytic Reaction (Table 4, entry 8). In the glovebox, (*S*)-$Me_2Si(OHF)(Cp-(-)$-menthyl)$SmN(TMS)_2$ (14.6 mg, 19.6 μmol) was weighed into a 5-mm NMR tube equipped with a Teflon valve (J-Young). The tube was then removed from the glovebox and attached to the high vacuum line. On the vacuum line, cyclohexane-d_{12} (0.5 mL) was vacuum-transferred and the tube was evacuated while the cyclohexane solution was frozen at $-78°$ C. Substrate **5** (0.05 mL of a 1.9 M solution in C_6D_6, 5-fold molar excess) was added via syringe under an Ar flush. The tube was next evacuated and backfilled with Ar 3 times while frozen at -78 °C. The tube was then sealed and thawed while shaking briefly (2 min) to afford a homogeneous light-yellow solution. The NMR tube was then immersed in an ice/water bath and kept at 0 °C for 45 days until the color of the solution changed from light yellow to orange. Although the melting point of pure C_6D_{12} is +4.75 °C, the reaction mixture was never observed to be frozen, presumably because of freezing point depression. After the reaction was complete, the reaction mixture was diluted with Et_2O (1.5 mL), filtered through a short pad of silica gel, rinsed with Et_2O (5 mL), and concentrated on a rotary evaporator at 0 °C to give crude product **6a/b** (95:5 by GC–MS) as a pale-yellow oil.

Preparative-Scale Catalytic Reactions (Method 1; in Situ Protection of Product, Table 1, entry 10). In the glovebox, (*S*)-$Me_2Si(OHF)$-$(Cp-(-)$-menthyl)$SmN(TMS)_2$ (34.1 mg, 45.8 μmol) was loaded into a 15-mL storage tube equipped with a magnetic stir bar and J. Young valve and dissolved in C_6D_6 (3 mL). The initial color of the catalyst solution was orange. Next, 0.50 mL of a solution of **5** in C_6D_6 (1.73 M, 0.87 mmol) was added to the catalyst solution via syringe. The color of the solution changed to light yellow upon the addition of **5**. The tube was then sealed and removed from the glovebox. The solution was stirred at room temperature for 8 days until the color turned back to orange. The reaction mixture was next cooled to 0 °C, diluted with Et_2O (2 mL), and quenched with 2 N NaOH (1.5 mL). Then, benzyl chloroformate (Cbz-Cl) (0.21 mL, 1.5 mmol) was added dropwise, and the mixture was allowed to warm to room temperature and stirred vigorously for 1 h. Next, the aqueous layer was separated and extracted with Et_2O (3 × 5 mL). The combined organic layers were washed with brine (5 mL), dried over $MgSO_4$, filtered, and concentrated to afford the crude Cbz-protected amine as a pale yellow oil. The crude product was purified by flash column chromatography (silica gel, hexanes/Et_2O = 6:1) to afford 203.7 mg (0.79 mmol, 91% yield) of **Cbz-6a/b** (97:3 *E/Z* mixture) as a colorless, clear oil.

Preparative-Scale Catalytic Reactions (Method 2, Table 1, entry 8). In the glovebox, $CGCSmN(TMS)_2$ (15.3 mg, 27.3 μmol) was loaded into a 15-mL storage tube equipped with a magnetic stir bar and J. Young valve and dissolved in C_6D_6 (3 mL). Next, **3** (89.5 mg) was weighed into a vial and dissolved in C_6D_6 (0.6 mL). The resulting solution was transferred to the catalyst solution using a pipet and rinsed with C_6D_6 (0.4 mL). The tube was then sealed and removed from the glovebox. The solution was then heated in an oil bath at 60 °C for 18 h. The reaction was then allowed to cool to room temperature, the solvent was removed on a rotary evaporator, and the crude yellow liquid was purified by flash column chromatography (silica gel, hexanes/EtOAc = 8:1) to afford 63.5 mg (71% yield) of **4a/b** as a slightly yellow liquid.

2-[(*E*)-Prop-1-enyl]pyrrolidine (2a).[11b] ^{1}H NMR (400 MHz, C_6D_6) δ 5.53 (d of quartet, 15.6 Hz, 5.6 Hz, 1H), 5.46 (dd, 15.6 Hz, 6.8 Hz), 3.36 (dt, 7.2 Hz, 6.8 Hz, 1H), 2.90–2.84 (m, 1H), 2.69–2.62 (m, 1H), 1.75–1.67 (m, 1H), 1.58 (d, 5.6 Hz, 3H), 1.61–1.42 (m, 2H), 1.35–

(20) Pangborn, A. B.; Giardello, M. A.; Grubbs, R. H.; Rosen, R. K.; Timmers, F. J. *Organometallics* **1996**, *15*, 1518–1520.

1.26 (m, 1H), 1.04 (br s, 1H); ^{13}C NMR (125.7 MHz, C$_6$D$_6$) δ 135.9, 124.7, 61.5, 47.1, 33.2, 26.0, 18.2. MS (rel abundance): M$^+$ 111.1 (14), 110.1 (22), 96.1 (73), 83.1 (11), 82.1 (13), 70.1 (38), 68.1 (100), 67.1 (12), 41.1 (25), 39.1 (18). HRMS-EI (*m/z*): [M$^+$] calcd for C$_7$H$_{13}$N, 111.1048; found, 111.1047.

2-[(Z)-Prop-1-enyl]pyrrolidine (2b).[11b] ^{13}C NMR (125.7 MHz, C$_6$D$_6$) δ 135.7, 124.5, 56.0, 47.3, 33.4, 26.3, 13.7. MS (rel abundance): M$^+$ 111.1 (14), 110.1 (22), 96.1 (73), 83.1 (11), 82.1 (13), 70.1 (38), 68.1 (100), 67.1 (12), 41.1 (25), 39.1 (18).

2-(Prop-2-enyl)pyrrolidine (2c). ^{13}C NMR (125.7 MHz, C$_6$D$_6$) δ 137.5, 116.3, 59.0, 41.7, 31.8, 26.2, 26.0. MS (rel abundance): [M − 41]$^+$ 70.1 (100), 68.1 (11), 43.1 (10), 41.1 (12).

N-Boc-2-[prop-1-enyl]pyrrolidine (Boc-2a/b).[21] ^{1}H NMR (500 MHz, CDCl$_3$) δ 5.48 (br s, 1H), 5.35 (br s, 1H), 4.53 (br s, 0.4H), 4.29 and 4.17 (br s, 0.6H), 3.38 (br s, 2H), 2.10−1.75 (m, 3H), 1.70 (d, 6.0 Hz, 3H), 1.64−1.58 (m, 1H), 1.44 (s, 9H). Both isomers exhibit indistinguishable mass spectra; MS (rel abundance): M$^+$ 211.2 (1), 155.1 (56), 140.1 (100), 138.1 (20), 114.1 (15), 110.1 (13), 96.1 (38), 83.1 (10), 70.1 (15), 68.1 (22), 67.1 (15), 57.1 (100), 56.1 (10), 55.1 (14), 43.0 (13), 42.0 (11), 41.1 (66), 39.0 (28). HRMS-EI (*m/z*): [M$^+$] calcd for C$_{12}$H$_{21}$NO$_2$, 211.1572; found, 211.1571.

N-Boc-2-(prop-2-enyl)pyrrolidine (Boc-2c).[21] ^{1}H NMR (500 MHz, CDCl$_3$) δ 5.75 (m, 1H), 5.06 (d, 16.5 Hz, 1 H), 5.03 (d, 8.5 Hz, 1H), 3.87 and 3.77 (br s, 1H), 3.40 and 3.32 (br s, 2H), 2.55 and 2.43 (br s, 1H), 2.14 and 2.11 (t, 8.0 Hz, 1H), 1.94−1.69 (m, 4H), 1.47 (s, 9H). MS (rel abundance): [M − 41]$^+$ 170.1 (9), 114.1 (65), 70.1 (100), 57.1 (84), 41.1 (40), 39.1 (13).

N-Bn-2-[(E)-prop-1-enyl]pyrrolidine (4a). (Isolated by the preparative-scale method 2) ^{1}H NMR (400 MHz, CDCl$_3$): δ 7.38−7.23 (m, 5H), 5.66 (d of quartet, 15.0 Hz, 6.4 Hz, 1H), 5.44 (ddd, 15.0 Hz, 8.2 Hz, 1.2 Hz, 1H), 4.07 (d, 12.8 Hz, 1H), 3.05 (d, 12.8 Hz, 1H), 2.95 (dt, 2.0 Hz, 8.2 Hz, 1H), 2.75 (quartet, 8.0 Hz, 1H), 2.09 (quartet, 8.8 Hz, 1H), 2.01−1.88 (m, 1H), 1.83−1.52 (m, 3H), 1.75 (d, 6.4 Hz, 3H); ^{13}C NMR (100.6 MHz, CDCl$_3$) δ 139.7, 133.8, 129.1, 128.2, 127.8, 126.7, 68.0, 58.4, 53.5, 31.9, 22.2, 18.2. MS (rel abundance): M$^+$ 201.2 (17), 200.2 (13), 186.1 (20), 172.1 (12), 160.1 (29), 158.1 (13), 91.1 (100), 82.1 (16), 65.1 (22), 41.1 (16), 39.0 (15). HRMS-EI (*m/z*): [M$^+$] calcd for C$_{14}$H$_{19}$N, 201.1518; found, 201.1511.

2-[(E)-Prop-1-enyl]piperidine (6a).[11b] ^{1}H NMR (500 MHz, C$_6$D$_6$) δ 5.56−5.48 (m, 2H), 2.92−2.87 (m, 2H), 2.46 (dt, 11.5 Hz, 7.5 Hz, 1H), 1.68−1.64 (m, 1H), 1.60−1.54 (m, 1H), 1.57 (d, 4.5 Hz, 3H), 1.42−1.36 (m, 2H), 1.32−1.18 (m, 2H), 1.00 (s, 1H); ^{13}C NMR (125.7 MHz, C$_6$D$_6$): δ 136.9, 124.4, 60.0, 47.7, 34.0, 26.9, 25.7, 18.3. MS (rel abundance): M$^+$ 125.1 (16), 124.1 (13), 110.1 (55), 97.1 (27), 96.1 (29), 84.1 (37), 82.1 (100), 83.1 (13), 69.0 (15), 68.1 (87), 67.1 (20), 56.1 (18), 55.0 (17), 54.0 (23), 53.0 (16), 44.0 (26), 43.0 (28), 42.0 (19), 41.0 (47), 40.0 (20), 39.0 (48). HRMS-EI (*m/z*): [M$^+$] calcd for C$_8$H$_{15}$N, 125.1205; found, 125.1204.

N-Boc-2-[(E)-prop-1-enyl]piperidine (Boc-6a). ^{1}H NMR (500 MHz, CDCl$_3$): δ 5.50 (d of quartet, 16.0 Hz, 6.0 Hz, 1H), 5.44 (dd, 16.0 Hz, 4.0 Hz, 1H), 4.73 (s, 1H), 3.92 (d, 13.0 Hz, 1H), 2.83 (dt, 2.5 Hz, 13.0 Hz, 1H), 1.70 (d, 5.5 Hz, 3H), 1.67−1.49 (m, 5H), 1.46 (s, 9H), 1.43−1.34 (m, 1H); ^{13}C NMR (125.7 MHz, CDCl$_3$) δ 155.6, 129.6, 126.6, 79.3, 52.1, 39.9, 29.7, 28.7, 25.9, 19.7, 18.1. MS (rel abundance): M$^+$ 225.1 (1), 170.1 (10), 169.1 (100), 154.1 (73), 152.1 (27), 141.1 (15), 128.1 (22), 124.1 (61), 110.1 (33), 97.1 (46), 96.1 (11), 84.1 (16), 82.1 (28), 68.1 (17), 67.1 (13), 57.1 (97), 56.1 (13), 55.1 (22), 43.1 (10), 41.1 (47), 39.1 (17). HRMS-EI (*m/z*): [M$^+$] calcd for C$_{13}$H$_{23}$NO$_2$, 225.1729; found, 225.1729.

N-Cbz-2-[(E)-prop-1-enyl]piperidine (Cbz-6a). (Isolated by preparative-scale method 1) ^{1}H NMR (500 MHz, CDCl$_3$) δ 7.43−7.28 (m, 5H), 5.61−5.45 (m, 2H), 5.17 and 5.13 (AB quartet, 12.5 Hz, 2H), 4.84 (s, 1H), 4.03 (d, 13.0 Hz, 1H), 2.92 (t, 12.0 Hz, 1H), 1.70 (d, 4.5

Hz, 3H), 1.78−1.49 (m, 5H), 1.48−1.34 (m, 1H); ^{13}C NMR (125.7 MHz, CDCl$_3$) δ 155.9, 137.3, 129.2, 128.6, 128.0, 127.9, 127.1, 67.1, 52.4, 40.2, 29.6, 25.8, 19.6, 18.1. IR (neat) 3063, 3030, 2937, 2857, 1703, 1497, 1445, 1421, 1351, 1355, 1323, 1257. MS (rel abundance): M$^+$ 259.2 (1), 168.1 (37), 124.1 (20), 92.1 (8), 91.1 (100), 82.1 (9), 65.1 (15), 55.1 (10). HRMS-EI (*m/z*): [M$^+$] calcd for C$_{16}$H$_{21}$NO$_2$, 259.1572; found, 259.1572. Anal. Calcd for C$_{16}$H$_{21}$NO$_2$: C, 74.10; H, 8.16; N, 5.40. Found: C, 73.88; H, 8.23; N, 5.34.

3,3-Dimethyl-6-[(E)-prop-1-enyl]piperidine (8a). ^{1}H NMR (500 MHz, CDCl$_3$) δ 5.57 (dq, 15.5 Hz, 6 Hz, 1H), 5.46 (dd, 15.5 Hz, 6 Hz, 1H), 2.92−2.89 (m, 1H), 2.59 (dd, 12 Hz, 2 Hz, 1H), 2.46 (d, 12 Hz, 1H), 1.65 (d, 6 Hz, 3H), 1.48−1.22 (m, 4H), 0.97 (s, 3H), 0.83 (s, 3H); ^{13}C NMR (125.7 MHz, CDCl$_3$) δ 135.0, 124.9, 59.0, 58.7, 37.9, 29.8, 29.4, 23.9, 18.1. MS (rel abundance): M$^+$ 153 (31), 138 (97), 125 (25), 110 (58), 96 (30), 82 (51), 70 (77), 68 (100), 67 (38), 55 (29), 41 (51). HRMS-EI (*m/z*): [M$^+$] calcd for C$_{10}$H$_{19}$N, 153.1518; found, 153.1523.

N-Boc-2-[(E)-but-1-enyl]pyrrolidine (Boc-10a). ^{1}H NMR (400 MHz, CDCl$_3$): δ 5.49 (br s, 1H), 5.32 (br s, 1H), 4.32 and 4.17 (br s, 1H), 3.38 (br s, 2H), 2.07−1.92 (m, 1H), 2.03 (quintet, 7 Hz, 2H), 1.90−1.73 (m, 2H), 1.70−1.64 (m, 1H), 1.44 (s, 9H), 0.98 (t, 7 Hz, 3H); ^{13}C NMR (125.7 MHz, CDCl$_3$): δ 155.4, 132.2, 129.8, 79.1, 58.9, 46.4, 32.8, 28.7, 25.4, 23.2, 14.0. MS (rel abundance): M$^+$ 225.2 (1), 169.1 (17), 152.1 (17), 140.1 (100), 114.1 (57), 108.1 (9), 96.1 (30), 70.1 (14), 68.1 (11), 67.1 (14), 57.1 (78), 55.1 (11), 43.0 (9), 41.0 (45), 39.0 (16). HRMS-EI (*m/z*): [M$^+$] calcd for C$_{13}$H$_{23}$NO$_2$, 225.1729; found, 225.1727.

N-Boc-2-(but-2-enyl)pyrrolidine (Boc-10c/d). *E/Z* = 76:24 mixture. ^{1}H NMR (400 MHz, CDCl$_3$) δ 5.56−5.31 (m, 2H), 3.79−3.71 (m, 1H), 3.40−3.20 (m, 2H), 2.45 (br s, 0.5H), 2.32 (br s, 0.5H), 2.05−1.98 (m, 1H), 1.85−1.74 (m, 3H), 1.72−1.62 (m, 1H), 1.65 (d, 6.0 Hz, 3H), 1.46 (s, 9H); ^{13}C NMR (125.7 MHz, CDCl$_3$) δ 155.3, 127.9, 127.6, 126.8, 126.2, 79.1, 57.3, 46.9, 46.5, 37.9, 37.1, 30.3, 29.3, 28.8, 23.8, 23.1, 18.3, 13.0. Both isomers exhibit indistingishable mass spectra; MS (rel abundance): [M − 55]$^+$ 170.1 (17), 152.1 (11), 114.1 (88), 70.1 (100), 57.1 (83), 55.1 (12), 41.1 (37), 39.0 (13).

2-[3-Phenyl-(E)-prop-2-enyl]pyrrolidine (12c). ^{1}H NMR (400 MHz, CDCl$_3$) δ 7.36 (d, 8.0 Hz, 2H), 7.30 (t, 7.4 Hz, 2H), 7.21 (t, 7.0 Hz, 1H), 6.46 (d, 16.0 Hz, 1H), 6.24 (dt, 16.0 Hz, 7.2 Hz, 1H), 3.14 (quintet, 6.8 Hz, 1H), 3.06−2.98 (m, 1H), 2.88−2.82 (m, 1H), 2.37 (t, 6.6 Hz, 2H), 1.95−1.86 (m, 1H), 1.84−1.66 (m, 3H), 1.43−1.34 (m, 1H); ^{13}C NMR (100.6 MHz, CDCl$_3$) δ 137.6, 131.7, 128.5, 128.1, 127.1, 126.1, 59.0, 46.7, 40.1, 31.5, 25.6. MS (rel abundance): [M − 70]$^+$ 117.1 (5), 115.1 (9), 91.1 (5), 71.1 (5), 70.1 (100), 43.1 (5). HRMS-CI (*m/z*): [MH$^+$] calcd for C$_{13}$H$_{18}$N, 188.1439; found, 188.1437.

***trans*-2-Methyl-5-[(E)-prop-1-enyl]pyrrolidine (*trans*-14a).** ^{1}H NMR (500 MHz, C$_6$D$_6$) δ 5.50 (d of quartet, 15.3 Hz, 5.5 Hz, 1H), 5.44 (dd, 15.3 Hz, 6.5 Hz, 1H), 3.64 (quartet, 6.5 Hz, 1H), 3.19 (sextet, 6.5 Hz, 1H), 1.89−1.82 (m, 1H), 1.80−1.74 (m, 1H), 1.58 (d, 5.5 Hz, 3H), 1.39 (d of quartet, 12.0 Hz, 8.5 Hz, 1H), 1.12 (d of quartet, 12.0 Hz, 8.5 Hz, 1H), 1.05 (m, 1 H), 1.00 (d, 6.5 Hz, 3H); ^{13}C NMR (125.7 MHz, C$_6$D$_6$) δ 136.6, 124.0, 60.4, 53.6, 34.9, 34.0, 23.0, 18.2. MS (rel abundance): M$^+$ 125.1 (11), 124.1 (8), 110.1 (52), 93.1 (8), 84.1 (15), 82.1 (100), 68.0 (18), 67.1 (15), 55.1 (8), 53.0 (8), 44.0 (8), 42.0 (16), 41.0 (26), 39.0 (25). HRMS-EI (*m/z*): [M$^+$] calcd for C$_8$H$_{15}$N, 125.1205; found, 125.1191.

N-Boc-*trans*-2-methyl-5-propylpyrrolidine (*trans*-17). *Trans:cis* = 9:1 mixture, ^{1}H NMR (500 MHz, CDCl$_3$) δ 3.97−3.64 (m, 2H), 2.05−1.76 (m, 3H), 1.61 (quartet, 6.0 Hz, 2H), 1.46 (s, 9H), 1.32−1.10 (m, 6H), 0.91 (t, 7.0 Hz, 3H); ^{13}C NMR (125.7 MHz, CDCl$_3$) δ 154.2, 154.1, 78.9, 57.8, 57.6, 54.1, 53.1, 53.0, 36.4, 35.3, 30.7, 29.9, 28.8, 27.6, 26.6, 20.6, 20.2, 20.1, 19.8, 19.6, 14.4, 14.3. Both isomers exhibit indistinguishable mass spectra; MS (rel abundance): M$^+$ 227.2 (1), 184.1 (16), 154.1 (16), 128.1 (100), 84.1 (84), 69.1 (10), 57.1 (83), 56.1 (10), 55.1 (14), 43.1 (11), 42.1 (11), 41.1 (50), 39.0 (14). HRMS-EI (*m/z*): [M$^+$] calcd for C$_{13}$H$_{25}$NO$_2$, 227.1886; found, 227.1888.

---

(21) Presumably, two possible conformers (pseudoequatorial or pseudoaxial propenyl) exist which interconvert slowly on the NMR time scale; therefore, some peaks appear as a pair.

***cis*-2-Methyl-6-[(*E*)-Prop-1-enyl]piperidine, (±)-Pinidine (*cis*-16a).**[11b,22] ^{1}H NMR (500 MHz, CDCl₃): δ 5.56 (d of quartet, 15.3 Hz, 6.5 Hz, 1 H), 5.45 (ddd, 15.3 Hz, 6.8 Hz, 1.5 Hz, 1H), 3.05−3.02 (m, 1H), 2.68−2.62 (m, 1H), 1.78−1.74 (m, 1H), 1.65 (d, 6.0 Hz, 3H), 1.59−1.54 (m, 2H), 1.40−1.28 (m, 2H), 1.20−0.98 (m, 2H), 1.05 (d, 6.0 Hz, 3H); ^{13}C NMR (125.7 MHz, CDCl₃) δ 135.3, 125.0, 59.6, 52.3, 34.0, 32.4, 24.8, 23.2, 18.0. MS (rel abundance): M⁺ 139.1 (35), 138.1 (18), 124.1 (100), 111.1 (21), 110.1 (20), 98.1 (23), 96.1 (64), 82.1 (56), 81.1 (39), 70.1 (22), 69.1 (13), 68.1 (54), 67.1 (20), 55.1 (20), 53.1 (12), 44.1 (30), 43.1 (13), 42.1 (21), 41.1 (33), 39.1 (20). HRMS-EI (*m/z*): [M⁺] calcd for C₉H₁₇N, 139.1361; found, 139.1357.

N-Boc-*cis*-2-methyl-6-propylpiperidine, (±)-*N*-Boc-dihydropinidine (*cis*-18).[23] ^{1}H NMR (500 MHz, CDCl₃) δ 4.31−4.28 (m, 1H), 4.08−4.04 (m, 1H), 1.69−1.24 (m, 10H), 1.46 (s, 9H), 1.16 (d, 7.5 Hz, 3H), 0.92 (t, 7.0 Hz, 3H); ^{13}C NMR (100.6 MHz, CDCl₃) δ 155.4, 79.0, 50.4, 45.9, 37.6, 30.6, 28.9, 27.7, 21.1, 20.7, 14.6, 14.5. MS (rel abundance): M⁺ 241.2 (0.1), 198.1 (10), 168.1 (8), 143.1 (8), 142.1 (100), 98.1 (46), 69.1 (8), 57.1 (40), 55.1 (10), 41.1 (21). HRMS-EI (*m/z*): [M⁺] calcd for C₁₄H₂₇NO₂, 241.2042; found, 241.2042.

N-Boc-*trans*-2-methyl-6-propylpiperidine, (±)-*N*-Boc-epidihydropinidine (*trans*-18).[24] ^{1}H NMR (500 MHz, CDCl₃): δ 3.93−3.90 (m, 1H), 3.88−3.79 (m, 1H), 1.70−1.22 (m, 10H), 1.46 (s, 9H), 1.23 (d, 6.8 Hz, 3H), 0.91 (t, 7.2 Hz, 3H); ^{13}C NMR (100.6 MHz, CDCl₃) δ 155.4, 78.9, 51.6, 47.2, 36.9, 28.9, 27.2, 23.5, 21.2, 20.6, 14.5, 14.1. MS (rel abundance): [M − 43]⁺ 198.1 (7), 168.1 (7), 143.1 (8), 142.1 (100), 98.1 (54), 69.1 (8), 57.1 (62), 55.1 (11), 41.1 (23).

Determination of Enantiomeric Excess and Absolute Configuration. The enantiomeric excess values of entries 1 and 3 in Table 4 were determined by GC−MS analysis of the corresponding Mosher amides[25] of the hydrogenated products. The two diastereomers of the (*S*)-Mosher amides of 2-propylpyrrolidine showed retention times of 33.5 and 34.2 min. The conditions were as follows: injector, 250 °C; initial oven temperature, 40 °C for 3 min; 20 °C/min to 150 °C, hold for 50 min; then 40 °C/min to 270 °C.

The values for the enantiomeric excess in entries 5−16 of Table 4 were determined by chiral stationary phase HPLC using a Regis (S,S)-Whelk O1 column (i.d. = 4.6 mm, length = 250 mm, particle size = 5 μm) with a flow rate of 2.0 mL/min and hexane/*i*PrOH (85:15) as eluent.[26] Racemic **6a** (Table 1, entry 9) was used as a standard, and two enantiomers of *N*-1-naphthoyl derivatives[26c] of racemic **6a** showed retention times of 23.5 and 43.0 min. The products from the enantioselective hydroamination (Table 4, entries 5−12) showed a minor peak at 23.5 min and major peak at 43.0 min. To assign the absolute configuration of the enantiomers, Cbz derivative of **6a** (**Cbz-6a**) was hydrogenated (H₂, Pd/C, EtOH, rt, 1 h) and then treated with HCl (2M in Et₂O) at 0 °C for 1 h to afford the HCl salt of 2-propylpiperidine (**25•HCl**), Coniine•HCl, in a 94% two-step overall yield (Scheme 3). The specific rotation value for this product was found to be [α]D²⁵ °C = +3.2° (EtOH, *c* 0.61). Compared to the known value [[α]D²⁰ °C = + 5.2° (EtOH, *c* 1.0) for (2*S*)-(+)-Coniine•HCl],[27] the configuration of the major enantiomer of 2-[(*E*)-prop-1-enyl]piperidine (**6a**) was assigned as *R*.

(2*S*)-2-Propylpiperidine, [(2*S*)-(+)-Coniine·HCl](25·HCl). 63% ee, ^{1}H NMR (500 MHz, CDCl₃) δ 9.51 (br s, 1H), 9.20 (br s, 1H), 3.45 (br s, 1H), 2.94 (br s, 1H), 2.81 (br s, 1H), 2.10−1.56 (m, 7H), 1.45 (br s, 3H), 0.95 (t, 7.0 Hz, 3H); ^{13}C NMR (125.7 MHz, CDCl₃) δ 57.5, 45.0, 35.6, 28.4, 22.7, 22.5, 18.9, 14.0. Anal. Calcd for C₈H₁₈ClN: C, 58.70; H, 11.08; N, 8.56. Found: C, 58.59; H, 10.94; N, 8.42. [α]D²⁵ °C = +3.2° (EtOH, *c* 0.61).

Kinetic Studies of Hydroamination/Cyclization. In a typical experiment, an NMR sample was prepared as described above (see Typical NMR-Scale Catalytic Reaction) but maintained at −78 °C until kinetic measurements were begun. The sample tube was then inserted into the probe of the INOVA-500 spectrometer which had been previously set to the appropriate temperature (*T* ± 0.2 °C; checked with a methanol or ethylene glycol temperature standard). A long pulse delay (8 s) was used during data acquisition to avoid saturation. The reaction kinetics were usually monitored from intensity changes in one of the conjugated olefinic resonances over three or more half-lives. The substrate concentration, C, was measured from the olefinic peak area, A_s, standardized to the area A_1 of the free EH(TMS)₂ (E = N or CH) formed as turnover commences. The EH(TMS)₂ is present as a result of quantitative protonolytic ligand cleavage during catalyst generation. Usually, data collected up to 80% conversion could be convincingly fit by least-squares to eq 3 where C_o is the initial concentration of substrate ($C_o = A_{so}/A_{1o}$). The turnover frequency (h⁻¹) was calculated from the least-squares determined slope (m) according to eq 4.

$$C = mt + C_o \tag{3}$$

$$N_t \ (\mathrm{h}^{-1}) = -(60 \ \mathrm{min \ h}^{-1})m \tag{4}$$

Results

The goal of this study was to further explore the scope and selectivity of the organolanthanide-mediated intramolecular hydroamination/cyclization reaction, searching for highly stereoselective catalytic pathways general to heterocycle construction. First, the catalytic intramolecular hydroamination/cyclization of the aminodienes is described, including the scope of the reaction, as well as the effects of varying substrate substituents, metal center, and ancillary ligands. Next, diastereo- and enantioselectivity are examined with an emphasis on alkaloid synthetic applications. Finally, reaction kinetics and mechanistic pathways are discussed, including rate laws, activation parameters, and their mechanistic implications.

Scope of Catalytic Aminodiene Hydroamination/Cyclization. Anaerobic cyclization of conjugated aminodienes[28] mediated by Cp′₂LnCH(TMS)₂ (Cp′ = η⁵-Me₅C₅),[16c] CGCLnN-(TMS)₂ (CGC = Me₂Si(η⁵-Me₄C₅)(*t*BuN)),[8g] or (*S*)-Me₂Si(OHF)-(CpR*)SmN(TMS)₂ (OHF = η⁵-octahydrofluorenyl; Cp = η⁵-C₅H₃; R* = (−)-menthyl[9a] precatalysts proceeds with high conversions and reasonably rapid turnover frequencies at 25 or 60 °C (Table 1). The reaction scope includes five- and six-membered ring formation using primary and secondary amines, as well as monosubstituted and 1,4-disubstituted dienyl groups. The transformation exhibits very high regioselectivity.[29] Thus, 2-substituted pyrrolidines (Table 1, entries 1−8, 13−16) and piperidines (Table 1, entries 9−12) are formed via 5-exo and 6-exo cyclizations, respectively, and there is no evidence of alternative 6- or 7-endo cyclizations. Products **a/b** are obtained as major products (Table 1, entries 1−12) for *terminal* monosubstituted dienes; however, products **c/d** predominate when *1,4-disubstituted* substrates are employed (Table 1, entries 13−16).

(22) Oppolzer, W.; Merifield, E. *Helv. Chim. Acta* **1993**, *76*, 957−962.
(23) Beak, P.; Lee, W. K. *J. Org. Chem.* **1993**, *58*, 1109−1117.
(24) Takahata, H.; Kubota, M.; Takahashi, S.; Momose, T. *Tetrahedron: Asymmetry* **1996**, *7*, 3047−3054.
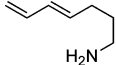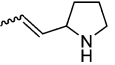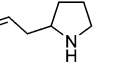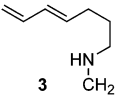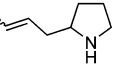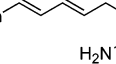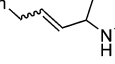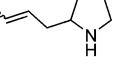(25) Dale, J. A.; Dull, D. L.; Mosher, H. S. *J. Org. Chem.* **1969**, *34*, 2543−2549.
(26) For examples of separation of racemates using an (S,S)-Whelk O1 column, see: (a) Pirkle, W. H.; Welch, C. J. *Tetrahedron: Asymmetry* **1994**, *5*, 777−780. (b) Pirkle, W. H.; Welch, C. J.; Lamm, B. *J. Org. Chem.* **1992**, *57*, 3854−3860. For an example of separation of 2-substituted piperidines, see: (c) Hyun, M. H.; Jin, J. S.; Lee, W. *Bull. Korean Chem. Soc.* **1997**, *18*, 336−339.
(27) Guerrier, L.; Royer, J.; Grierson, D. S.; Husson, H.-P. *J. Am. Chem. Soc.* **1983**, *105*, 7754−7755.
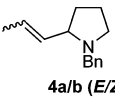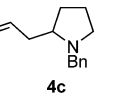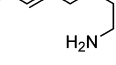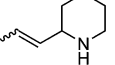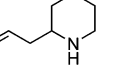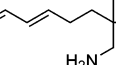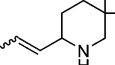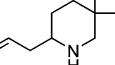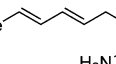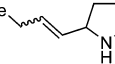
(28) See the Supporting Information for aminodiene substrate synthesis.
(29) Hydroamination/cylization of monosubstituted allenylamines affords mixtures of endo- and exo-cyclization regioisomers, whereas 1,3-disubstituted allenylamines exclusively yield the exo-cyclization product. See ref 11b.

Table 1. Results for Organolanthanide-Catalyzed Hydroamination/Cyclization of Conjugated Aminodienes

Entry	Substrate	Product	%Conv.[a] (Yield)	Ratio[c]	N_t, h^{-1} (°C)[d]
				a : b : c	
1.			> 95	84: 16: 0	40 (25)[e]
2.			> 95	72: 11: 17	0.79 (60)[f]
3.			93	30: 19: 51	0.05 (60)[g]
4.	**1**	**2a/b (E/Z)** **2c**	90	59: 41: 0	3.1 (25)[h]
5.			90	87: 13: 0	~0.08 (25)[i]
6.			> 95	98: 2: 0	74 (23)[j]
7.			> 95	93: 7: 0	12 (25)[k]
8.	**3** (HN–CH₂Ph)	**4a/b (E/Z)** (Bn) **4c** (Bn)	85 (71)[b]	87: 7: 6	5.8 (60)[h]
9.	**5**	**6a/b (E/Z)** **6c**	> 95	98 : 2: 0	3.0 (25)[e]
10.			> 95 (91)[b]	97 : 3: 0	0.11 (25)[k]
11.	**7**	**8a/b (E/Z)** **8c**	> 95	93 : 7: 0	21 (25)[e]
12.			> 95	96 : 4: 0	1.7 (25)[k]
				a : b : c : d	
13.	**9**	**10a/b (E/Z)** **10c/d (E/Z)**	94	38: 0: 47:15	1.8 (60)[e]
14.			93	23: 0: 72: 5	0.02 (60)[f]
15.	**11**	**12a/b (E/Z)** **12c/d (E/Z)**	92	>94% **c**	89 (60)[e]
16.			90	>94% **c**	2.3 (60)[f]

[a] Determined by ^{1}H NMR. [b] Preparative-scale yield (entry 8) or that of Cbz carbamate (entry 10). [c] Determined by ^{1}H NMR and GC−MS or GC−MS of Boc derivatives (entries 2, 3, 13, 14). [d] Turnover frequencies measured in C_6D_6 with 3−11 mol % precatalyst. [e] Cp′$_2$LaCH(TMS)$_2$ as precatalyst. [f] Cp′$_2$SmCH(TMS)$_2$ as precatalyst. [g] Cp′$_2$YCH(TMS)$_2$ as precatalyst. [h] CGCSmN(TMS)$_2$ as precatalyst. [i] CGCYN(TMS)$_2$ as precatalyst. [j] (S)-Me$_2$Si(Me$_4$Cp)(CpR*)SmN(TMS)$_2$ as precatalyst (R* = (−)-menthyl). [k] (S)-Me$_2$Si(OHF) (CpR*)SmN(TMS)$_2$ as precatalyst (R* = (−)-menthyl).

In marked contrast to aminoallene hydroaminations in which the Z double bond isomer (product **b**) is generally obtained as a major product,[11] good to high E double bond selectivity is observed with aminodienes. Monitoring the reactions by ^{1}H NMR shows that product ratio varies in only a minor way with conversion, in most cases. However, for cyclization of dienes **9** and **11**, the E/Z product distribution is time-dependent, ultimately favoring thermodynamic products. For conversion **11 → 12**, initial formation of **12a** and subsequent isomerization to **12c** is observed in situ by ^{1}H NMR. Presumably, the doubly activated benzylic/allylic C−H functionality in propenylpyrrolidine **12a** is sufficiently acidic to facilitate isomerization (eq 5). As observed for aminoalkene, aminoalkyne, and aminoallene

(5)
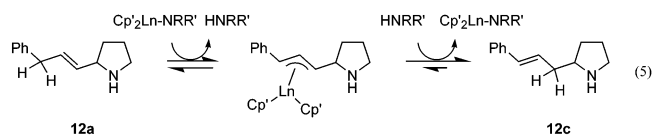
cyclizations, the ring-size dependence cyclization rates (N_t) for aminodienes are 5 > 6, consistent with the classical, stereo-electronically controlled cyclization process.[30] Geminal dimethyl

substitution of the carbon backbone (the Thorpe−Ingold effect,[31] Table 1, entries 11 and 12) increases the N_t's by approximately 1 order of magnitude, as also observed in aminoalkene hydroamination.[8j] Note that observed rates are comparable to or greater than those of 4-pentenamine and 5-hexenamine hydroamination/cyclization, despite increased substrate steric encumbrance (Table 2).

Metal and Ancillary Ligand Effects on Catalytic Aminodiene Hydroamination/Cyclization. In the case of amino-alkene hydroamination/cyclization, both increasing the Ln^{3+} ionic radius and opening the metal coordination sphere by *ansa*-fusion of the ancillary ligands (Cp′$_2$Ln− → Me$_2$SiCp″$_2$Ln− or Cp′$_2$Ln− → Me$_2$SiCp″(CpR*)Ln−; Cp″ = C$_5$Me$_4$, R* = (−)-menthyl)[32,9b] increases the turnover frequencies (N_t), presumably reflecting significant steric demands in the insertive transition state (Scheme 1, step i).[8j,9b,32] Catalyst structural effects qualitatively similar to those in monosubstituted alkenylamine

(30) (a) Carey, F. A.; Sundberg, R. J. *Advanced Organic Chemistry*, 4th ed.; Kluwer Academic/ Plenum Publishers: New York, 2000; Part A, Chapter 3.9. (b) Illuminati, G.; Mandoline, L. *Acc. Chem. Res.* **1981**, *14*, 95−102.
(31) (a) Eliel, E. L.; Wilen, S. H.; Mander, L. N. *Stereochemistry of Organic Compounds*; Wiley-Interscience: New York, 1994; pp 682−684. (b) Kirby, A. J. *Adv. Phys. Org. Chem.* **1980**, *17*, 183−278.
(32) Jeske, G.; Schock, L. E.; Mauermann, H.; Swepston, P. N.; Schumann, H.; Marks, T. J. *J. Am. Chem. Soc.* **1985**, *107*, 8103−8110.

**Table 2.** Rate Comparison for Aminoalkene and Aminodiene Hydroamination

	N_t, h^{-1} (°C)	
Substrate	Cp'$_2$LaCH(TMS)$_2$	(OHF*)SmN(TMS)$_2$[a]
(alkene-NH$_2$)	13 (25)[b]	2.6 (25)[c]
(alkene-NH$_2$)	~ 0.7 (120)[d]	—
(diene-NH$_2$)	40 (25)	12 (25)
(alkene-NH$_2$)	5 (60)[b]	6.6 (60)[c]
(alkene-NH$_2$)	3 (25)	0.11 (25)
(alkene-NH$_2$)	—	0.6 (25)[c]
(alkene-NH$_2$)	~ 4 (120)[d]	—
(diene-NH$_2$)	21 (25)	1.7 (25)

[a] OHF* = (S)-Me$_2$Si(η^5-octahydrofluorenyl)(CpR*), R*= (−)-menthyl. [b] Reference 8l. [c] Reference 9a. [d] Estimated from the reaction conditions (catalyst mol % and reaction time) reported in ref 8c.

hydroamination are also operative in the present case. Thus, for cyclization $1 \rightarrow 2$, N_t increases substantially with increasing metal ionic radius[8j,33] (Cp'$_2$La− > Cp'$_2$Sm− > Cp'$_2$Y−, and CGCSm− > CGCY−; Table 1, entries 1−3 and entries 4 and 5). Further examples of such dramatic N_t change from La to Sm are in the cyclization of $9 \rightarrow 10$ (N_t = 1.8 vs 0.02 h^{-1} at 60 °C; Table 1, entries 13 and 14), and $11 \rightarrow 12$ (N_t = 89 vs 2.3 h^{-1} at 60 °C; Table 1, entries 15 and 16). The kinetic effects of the supporting π-ligation on N_t for aminodiene hydroamination/cyclization were also probed for transformation $1 \rightarrow 2$, and N_t also generally increases with more open ligation [Me$_2$SiCp''-(CpR*) > Me$_2$Si(OHF)(CpR*) ≥ CGC ≫ Cp'$_2$; Table 1, entries 2, 4, 6, and 7]. Thus, aminodiene hydroamination/cyclization experiences an appreciable acceleration in rate when larger ionic radius Ln^{3+} catalysts or more open ligations such as Me$_2$SiCp''-(CpR*) or Me$_2$Si(OHF)(CpR*) are employed.

Diastereo- and Enantioselectivity in Aminodiene Hydroamination/Cyclization. Cyclization of 5-hexen-2-amine has been studied in detail for diastereoselectivity effects in aminoalkene hydroamination/cyclization (eq 6). It was found that


(6)
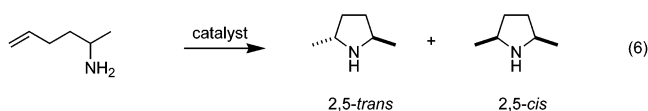
2,5-*trans*   2,5-*cis*

the 2,5-*trans*:2,5-*cis* ratio is highly dependent on lanthanide ion size, π-ancillary ligation, reaction temperature, and added exogenous ligands such as *n*-propylamine.[8j] For example, Cp'$_2$-Ln−/Me$_2$SiCp''$_2$Ln− (Ln = Nd, Sm) precatalysts afford only modest diastereoselection (1:1−5:1, *trans*/*cis*) at 25 °C, whereas CGCLn (Ln = Nd, Sm)[8g] and chiral catalysts Me$_2$SiCp''(CpR*)-Ln- (Ln = Nd, Sm, R* = (−)-menthyl)[9b] exhibit greatly improved diastereoselectivities (10:1 *trans*/*cis* and >95% *trans*, respectively). In contrast, aminoallene hydroamination/cyclization mediated by Cp'$_2$Ln− catalysts proceeds, depending on the substrate, with either exclusive 2,5-*trans* or 2,6-*cis* diastereo-

selectivity, making the methodology particularly attractive for pyrrolidine and pyrrolizidine alkaloid synthesis.[11]

In the present study, the ring substituent diastereoselectivity of aminodiene hydroamination/cyclization was investigated with α-methyl aminodiene substrates (Table 3). Good diastereoselectivities (9:1 = 2,5-*trans*/2,5-*cis*) are observed in the formation of a 2,5-*trans* disubstituted pyrrolidine ($13 \rightarrow 14$) when CGC-SmN(TMS)$_2$ or Me$_2$Si(OHF)(CpR*)SmN(TMS)$_2$ is used as a catalyst (Table 3, entries 2 and 3). The relatively modest rate and low selectivity with Cp'$_2$LaCH(TMS)$_2$ for reaction $13 \rightarrow$ 14 (Table 3, entry 1) is rather exceptional considering that Cp'$_2$-LaCH(TMS)$_2$ consistently exhibits high N_t's and good stereoselectivities with other aminodiene substrates. However, it was previously observed that Cp'$_2$LaCH(TMS)$_2$ is conspicuously ineffective in the hydroamination/cyclization of a similar substrate, 5-hepten-2-amine, at high temperatures, while it serves as the most effective catalyst for cyclization of other amine-tethered 1,2-disubstituted alkenes.[8c] In contrast, the present work reveals excellent diastereoselectivity in formation of a 2,6-*cis* disubstituted piperidine (Table 3, entries 4 and 5).[34] Thus, aminodiene 15 almost exclusively generates *cis*-2-methyl-6-[(E)-prop-1-enyl]pyrrolidine (*cis*-$16a$) in high yield with reasonable rate at room temperature. Note that entry 4 demonstrates a concise, efficient synthesis of (±)-pinidine[35] with excellent stereocontrols for both 2,6-*cis* substitution (*cis*/*trans* = 178:1) and *trans*-alkene geometry (E/Z/allyl = 94:1:5).

Enantioselective hydroamination/cyclizations were investigated by using the C_1-symmetric chiral organolanthanocene catalysts, (S)-Me$_2$SiCp''(CpR*)LnE(TMS)$_2$ (Ln = Sm, Y; E = N, CH; R* = (−)-menthyl)[9b,c] and (S)-Me$_2$Si(OHF)(CpR*)-SmN(TMS)$_2$,[9a] as well as the recently developed C_2-symmetric bisoxazoline catalyst, (4R,5S)-Ph$_2$BoxLa[N(TMS)$_2$]$_2$ (Table 4).[36]

(S)-Me$_2$SiCp''(CpR*)Ln   (S)-Me$_2$Si(OHF)(CpR*)Sm   (4R,5S)-Ph$_2$BoxLa
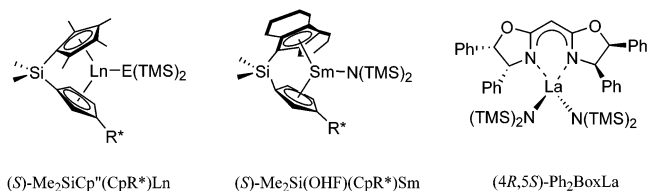
The enantioselectivities of the reactions were assayed by chiral HPLC analysis of the 1-naphthoyl amide derivatives[26c] of the crude products or hydrogenated products if the reaction produced >5% minor isomer. Distinctive color changes associated with catalytic initiation and termination as in hydroamination of other amino-unsaturation systems[8j,10c,11b] were found to be very useful for qualitatively monitoring the course of the reaction, especially at 0 °C. Thus, the original orange solution of the paramaganetic Sm^{3+} (4f ^{5}) precatalyst, Me$_2$Si(OHF)(CpR*)SmN(TMS)$_2$, immediately turns to the light yellow color upon substrate addition. The resulting reaction solution reverts to the original color upon aminodiene substrate consumption. In the case of heptadienyl substrate 1 for pyrrolidine formation, the results indicate modest selectivity (17−41% ee; Table 4, entries 1−4) at best, less than

(33) Representative eight-coordinate effective ionic radii: La(III), 1.160 Å; Nd-(III), 1.109 Å; Sm(III), 1.079 Å; Y(III), 1.019 Å; Yb(III), 0.985 Å; Lu-(III), 0.977 Å. See: Shannon, R. D. *Acta Crystallogr., Sect. A* **1976**, *A32*, 751−767.

(34) Relative stereochemistry confirmed by NOESY experiments and derivatization.

(35) Kirihara, M.; Nishio, T.; Yokoyama, S.; Kakuda, H.; Momose, T. *Tetrahedron* **1999**, *55*, 2911−2926 and references therein.

(36) (a) Hong, S.; Ryu, J.-S.; Tian, S.; Metz, M. V.; Marks, T. J. *Abstracts of Papers*; communicated in part at the 224th National ACS Meeting, Boston, MA; August 2002; American Chemical Society: Washington, DC, 2002; abstract INOR 668. (b) Hong, S.; Tian, S.; Metz, M. V.; Marks, T. J. *J. Am. Chem. Soc.*, in press.

Table 3. Diasteroselectivity in the Organolanthanide-Catalyzed Hydroamination/Cyclization of Conjugated Aminodienes[a]

Entry	Substrate	Product	Ratio[b]	N_t, h^{-1} (°C)[c]
			2,5-*cis* : 2,5-*trans*	
1.			42 : 58[d]	1.0 (25)[e]
2.			12 : 88	15 (25)[f]
3.	**13**	***cis*-14a/b *trans*-14a/b**	10 : 90	78 (25)[g]
			2,6-*cis* : 2,6-*trans*	
4.			99.4 : 0.6[h]	3.7 (25)[e]
5.			97 : 3	0.9 (25)[f]
6.	**15**	***cis*-16a/b *trans*-16a/b**	78 : 22	4.0 (60)[g]

[a] Starting aminodienes completely consumed as judged by ^{1}H NMR (>95% conversion). [b] Determined by GC−MS ratio of corresponding hydrogenated Boc derivatives. [c] Turnover frequencies measured in C_6D_6 with 5 mol % precatalyst. [d] Ca. 10% allyl products formed. [e] Cp'$_2$LaCH(TMS)$_2$ as precatalyst. [f] (*S*)-Me$_2$Si(OHF)(Cp*)SmN(TMS)$_2$ as precatalyst. [g] CGCSmN(TMS)$_2$ as precatalyst. [h] *Cis/trans* = 178:1; alkene isomer ratio (*E/Z*/allyl = 94:1:5).

**Table 4.** Enantioselective Cyclization of Aminodienes[a]

1 : n = 1, R= H
5 : n = 2, R= H
7 : n = 2, R= CH$_3$

2 : n = 1, R= H
6 : n = 2, R= H
8 : n = 2, R= CH$_3$
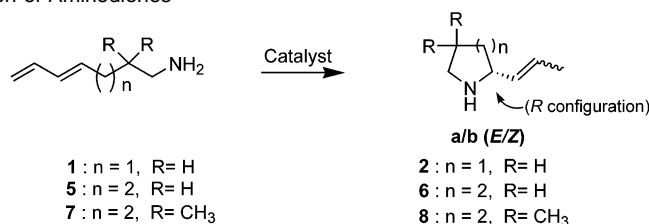
entry	substrate	product (ratio)[b]	chiral precatalyst	solvent	N_t, h^{-1}	temp (°C)	%ee[c] (config)[d]
1	**1**	**2a/b** (93:7)	OHF*Sm	benzene-d_6	12	25	23
2	**1**	**2a/b** (98:2)	Cp*Sm	benzene-d_6	74	23	25[e]
3	**1**	**2a/b** (98:2)	Cp*Y	benzene-d_6	0.09	25	41
4	**1**	**2a/b** (63:37)	Ph$_2$BoxLa	benzene-d_6	3.0	23	17[e]
5	**5**	**6a/b** (97:3)	OHF*Sm	benzene-d_6	0.11	25	63 (*R*)
6	**5**	**6a/b** (96:4)	OHF*Sm	toluene-d_8		0	64 (*R*)
7	**5**	**6a/b** (96:4)	OHF*Sm	cyclohexane-d_{12}	0.04	25	64 (*R*)
8	**5**	**6a/b** (95:5)	OHF*Sm	cyclohexane-d_{12}		0	69 (*R*)
9	**5**	**6a/b** (97:3)	OHF*Sm	methylcyclohexane-d_{14}	0.09	25	64 (*R*)
10	**5**	**6a/b** (97:3)	OHF*Sm	methylcyclohexane-d_{14}		0	71 (*R*)
11	**5**	**6a/b** (97:3)	OHF*Sm	pentane	∼0.08	25	65 (*R*)
12	**5**	**6a/b** (98:2)	Cp*Sm	benzene-d_6	0.1	25	37 (*R*)
13	**5**	**6a/b** (41:59)	Ph$_2$BoxLa	benzene-d_6	0.6	60	54[e] (*R*)
14	**7**	**8a/b** (96:4)	OHF*Sm	benzene-d_6	1.7	25	19
15	**7**	**8a/b** (93:7)	OHF*Sm	cyclohexane-d_{12}		0	24
16	**7**	**8a/b/c** (39:57:4)	Ph$_2$BoxLa	benzene-d_6	1.4	23	45[e]

[a] Conditions: 4−7 mol % or 20 mol % (0 °C reactions) catalyst, ∼0.6 mL of solvent. [b] Determined by GC−MS. [c] For the major isomer, determined by chiral HPLC analysis. Measured ee's vary only weakly with conversion. [d] Determined by optical rotation of the HCl salt of the hydrogenated product. Absolute configuration of major isomer. [e] Determined by chiral HPLC analysis of hydrogenated product.

that observed in homologous pentenamine cyclization with the same catalysts (40−69% ee; Table 5, entries 1−4).[9,36] Octadienamine cyclizations **5 → 6a/b** display higher selectivity, with the Me$_2$Si(OHF)(CpR*)Sm catalyst exhibiting the highest ee of 71% (Table 4, entries 5−13). This enantioselectivity represents a substantial improvement in the formation of 2-substituted piperidines versus the homologous aminoalkene cyclization mediated by the same OHF catalyst, affording only 10% ee at 60 °C (Table 5, entry 5). For cyclization **5 → 6a/b** mediated by the OHF catalyst in benzene at 25 °C, enantiomeric excess was assayed at different conversions, and measured ee's were found to vary only weakly with conversion (64% ee at 25% conversion, 64% ee at 47% conversion, 65% ee at 70% conversion). In an effort to further enhance ee's, several other nonpolar solvents (toluene, cyclohexane, methylcyclohexane, and pentane) were employed but only minor solvent effects on enantioselectivity were observed. Decreasing the temperature from 25 °C
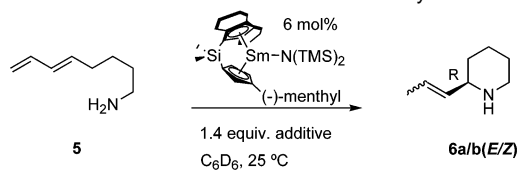
to 0 °C improves ee's by ∼5%. When exogenous chiral Lewis base ligands are added, enantioselectivity remains virtually the same or increases only slightly, while reaction rates are significantly depressed (Table 6). *Gem*-dimethyl substitution on the substrate carbon backbone enhances cyclization rates as expected;[31] however, the enantioselectivity is diminished (Table 4, entries 14−16). Scheme 3 illustrates how the absolute configuration of **6a/b** was determined. Note that the natural product (+)-coniine•HCl[37] is efficiently synthesized from prochiral aminodiene substrate **5** in an essentially two-step sequence in very high isolated yield. Although the enantioselection in the key hydroamination/cyclization step is not perfected yet with currently available chiral organolanthanide catalysts, this example demonstrates the potential synthetic

(37) For the catalytic asymmetric synthesis of coniine via imine hydrosilylation, see: Reding, M. T.; Buchwald, S. L. *J. Org. Chem.* **1998**, *63*, 6344−6347 and references therein for other recent syntheses.

Table 5. Enantioselective Cyclization of Homologous Aminoalkenes

19 : n = 1, R= H
21 : n = 2, R= H
23 : n = 2, R= CH₃

20 : n = 1, R= H
22 : n = 2, R= H
24 : n = 2, R= CH₃
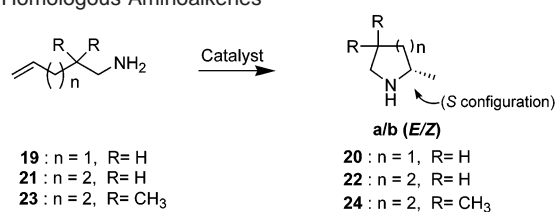
entry	substrate	product	chiral precatalyst	solvent	N_t, h⁻¹	temp (°C)	% ee^a (config)^b	ref
1	**19**	**20**	OHF*Sm	benzene-d_6	2.6	25	46 (+)	9a
2	**19**	**20**	Cp*Sm	pentane	33	25	62 (+)	9b
3	**19**	**20**	(R)-Cp*Y	pentane		25	69 (+)	9b
4	**19**	**20**	Ph₂BoxLa	benzene-d_6	0.09	23	40 (−)	43
5	**21**	**22**	OHF*Sm	benzene-d_6	6.6	60	10 (+)	9a
6	**23**	**24**	OHF*Sm	benzene-d_6	0.6	25	41 (+)	9a
7	**23**	**24**	Cp*Sm	pentane	2	25	15 (−)	9b
8	**23**	**24**	Ph₂BoxLa	benzene-d_6	4.0	60	56 (+)	43

^{a} Determined by GC-MS of the corresponding Mosher amide (entries 1, 5, 6), ^{19}F NMR of the Mosher amide (entries 2, 3, 7), or chiral HPLC analysis (entries 4, 8). ^{b} Determined by optical rotation.

Table 6. Effects of Chiral Lewis Base Additives on Enantioselective Aminodiene Hydroamination/Cyclization


additive					
product ratio (E/Z)	99: 1	99: 1	98: 2	98: 2	
N_t, h⁻¹	0.05	0.04	0.04	0.05	No reaction
%ee (config.)	65 (R)	65 (R)	65 (R)	65 (R)	

Scheme 3. Synthesis of (2S)-(+)-Coniine•HCl; Determination of the Absolute Configuration of **6a**
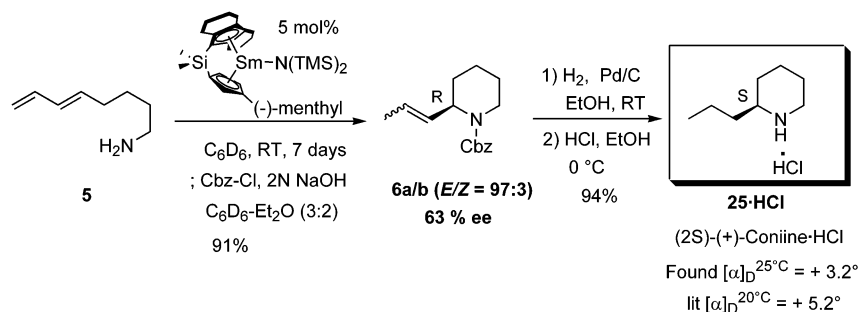
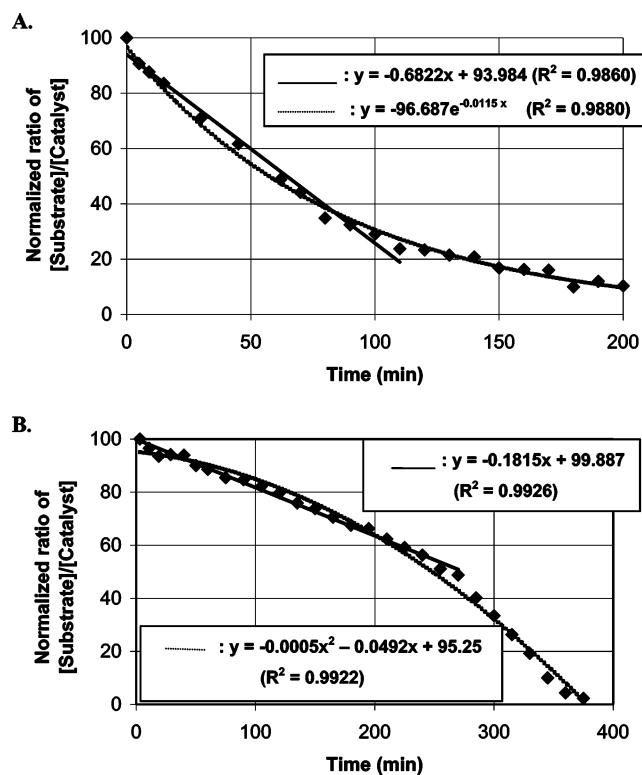utility of the enantioselective hydroamination routes to 2-substituted piperidines.

Kinetic and Mechanistic Studies of Aminodiene Hydroamination/Cyclization. A kinetic study of the **1→ 2a/b** cyclization was undertaken by in situ ^{1}H NMR spectroscopy. The reaction of a 40−80-fold molar excess of (4E,6)-heptadien-1-amine (**1**) with Cp′₂LaCH(TMS)₂ was monitored with constant catalyst concentration until complete substrate consumption. The decrease of one of the diene olefinic peaks ($\delta \approx 6.0$ ppm) was

normalized to the ^{1}H resonance of the stoichiometrically generated CH₂(TMS)₂ reaction byproduct ($\delta \approx 0.2$ ppm). Figure 2A presents kinetic data for this reaction (typical of many runs), which indicate that the reaction rate is zero order in substrate concentration over ∼3 half-lives, in analogy to the hydroamination/cyclization of aminoalkenes,[8j] aminoalkynes,[10c] and aminoallenes.[11b] Another example of such zero-order behavior is in the cyclization **15→ 16a/b** using the precatalyst CGCSmN-(TMS)₂ in benzene-d_6 at 60 °C (Figure 2B and Table 3, entry

A.

B.
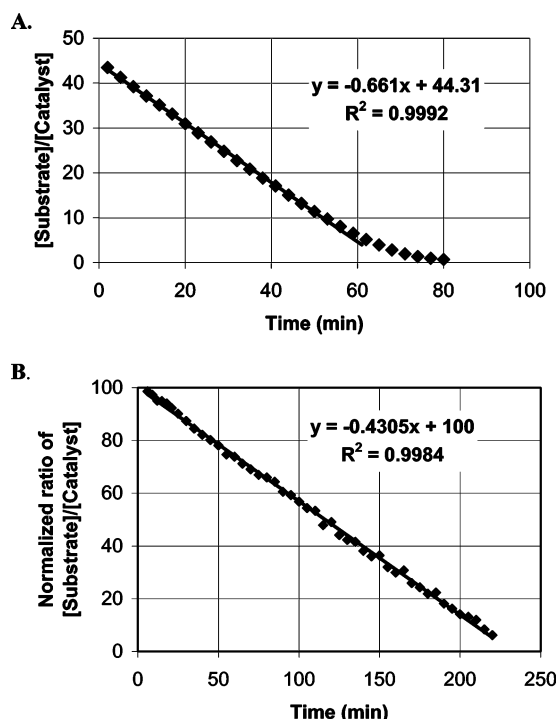
Figure 2. (A) Ratio of substrate to lanthanide concentration as a function of time for the hydroamination/cyclization of (4*E*,6)-heptadien-1-amine (**1**) using the precatalyst Cp′$_2$LaCH(TMS)$_2$ in benzene-d_6 at 25 °C. (B) Normalized ratio of substrate to lanthanide concentration as a function of time for the hydroamination/cyclization of (6*E*,8)-nonadien-2-amine (**15**) using the precatalyst CGCSmN(TMS)$_2$ in benzene-d_6 at 60 °C.

6). Indeed, many aminodiene cyclizations exhibit zero-order kinetics in substrate (Table 1, entries 1−3, 6, 7, 13−16; Table 3, entries 2, 5, 6). However, deviations from the zero-order linearity are also observed in some cases (Figure 3). Two variants are observed; either the rate of the aminodiene cyclization begins to decrease (Figure 3A) or increase (Figure 3B) after about the first half-life. The first type of deviation can be modeled by *competitive product inhibition*[8j,9b,38] (Table 1, entries 4 and 8; Table 3, entries 1, 3, 4), whereas the second type can be interpreted as *substrate self-inhibition* (Table 1, entries 9−12). Since the first type of kinetic plot can be fit very well over a broad range of conversions with an exponential function (Figure 3A), it is not straightforward to distinguish between zero-order kinetics with substantial competitive product inhibition and true first-order kinetics by this integrated rate law method alone. Therefore, the half-life method in conjunction with the initial rate method[39] was employed to determine the reaction order in aminodiene substrate concentration for the transformation **1→ 2a/b** using the CGCSmN(TMS)$_2$ precatalyst. Three new reactions starting with different initial substrate concentrations were analyzed by ^{1}H NMR. Instead of real half-life points for each run, projected half-life points from the first 20% conversion data were taken and plotted versus initial substrate concentration because of possible product participation in reaction rate (Figure 4A). Figure 4A shows that the half-life points increase linearly with initial substrate concentration,

(38) Organolanthanide-catalyzed hydrophosphinations exhibit similar but more pronounced kinetic inhibition effects, depending upon the steric bulk of the product. See: Douglass, M. R.; Stern, C. L.; Marks, T. J. *J. Am. Chem. Soc.* **2001**, *123*, 10221−10238.
(39) Steinfeld, J. I.; Francisco, J. S.; Hase, W. L. *Chemical Kinetics and Dynamics* 2nd ed.; Prentice Hall: New Jersey, 1999; pp 1−13.

A.

B.

Figure 3. (A) Normalized ratio of substrate to lanthanide concentration as a function of time for the hydroamination/cyclization of (4*E*,6)-heptadien-1-amine (**1**) using the precatalyst CGCSmN(TMS)$_2$ in benzene-d_6 at 25 °C. (B) Normalized ratio of substrate to lanthanide concentration as a function of time for the hydroamination/cyclization of (5*E*,7)-octadien-1-amine (**5**) using the precatalyst Cp′$_2$LaCH(TMS)$_2$ in benzene-d_6 at 25 °C.

clearly indicating zero-order kinetics in [substrate] (eqs 7 and 8).

$$-\frac{d[S]}{dt} = k[S]^n \qquad (7)$$

$$n = 0: \quad [S]_t = [S]_o - kt \qquad t_{1/2} = \frac{[S]_o}{2k} \qquad (8)$$

$$n = 1: \quad [S]_t = [S]_o e^{-kt} \qquad t_{1/2} = \frac{\ln 2}{k} \qquad (9)$$

$$\text{In general } (n \neq 1), \qquad t_{1/2} = \frac{(2^{n-1} - 1)}{k(n-1)[S]_o^{n-1}} \qquad (10)$$
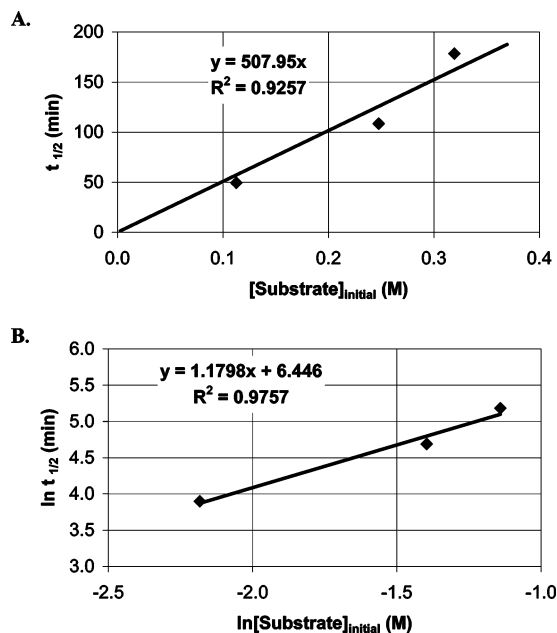
To further test the product inhibition hypothesis, an additional aliquot of **1** was added to the same reaction mixture, after the initial cyclization **1→ 2a/b** was complete by ^{1}H NMR (Figure 5). The measurement shows more severe inhibition (deviation from zero-order kinetics) in the second data set, where substantial concentrations of product **2a/b** are now present. Therefore, the observed deviation from linearity likely reflects product participation. Further discussion of this mechanistic implication is deferred to the Discussion section.

When the initial concentration of aminodiene is held constant and the concentration of the precatalyst is varied over a 10-fold range, a plot of reaction rate versus precatalyst concentration (Figure 6A) and a plot of ln(rate) versus ln[catalyst] (van't Hoff plot, slope = reaction order, Figure 6B) indicates the reaction

A.

$y = 507.95x$
$R^2 = 0.9257$

(x-axis: [Substrate]$_{initial}$ (M); y-axis: $t_{1/2}$ (min))

B.

$y = 1.1798x + 6.446$
$R^2 = 0.9757$

(x-axis: ln[Substrate]$_{initial}$ (M); y-axis: ln $t_{1/2}$ (min))

Figure 4. (A) Plot of half-life points projected from the initial 20% conversion as a function of initial substrate concentration for the hydroamination/cyclization of (4E,6)-heptadien-1-amine (**1**) using the precatalyst CGCSmN(TMS)$_2$ in benzene-d_6 at 25 °C. The line is the least-squares fit to the data points with *y*-intercept = 0. (B) Half-life method plot for the hydroamination/cyclization of (4E,6)-heptadien-1-amine (**1**) using the precatalyst CGCSmN(TMS)$_2$ in benzene-d_6 at 25 °C. The line is the least-squares fit to the data points. The slope of the line equals $1 - n$ (n = reaction order).

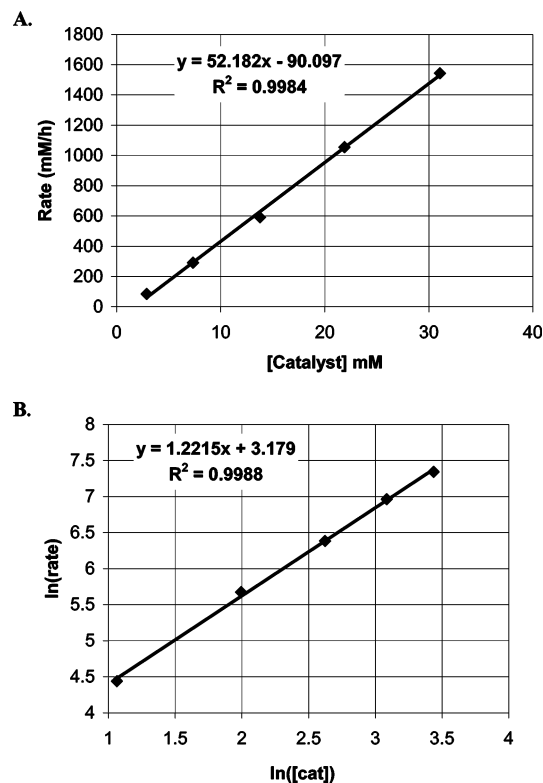(x-axis: Time (min); y-axis: Normalized [sub]/[cat]; labels: trial 1, trial 2)
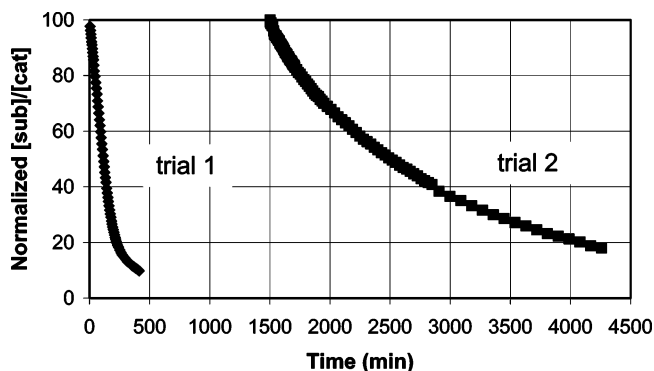
Figure 5. Normalized ratio of substrate to lanthanide concentration as a function of time for the hydroamination/cyclization of (4E,6)-heptadien-1-amine (**1**) using the precatalyst CGCSmN(TMS)$_2$ in benzene-d_6 at 25 °C. The deviation from zero-order kinetics is ascribed to competitive inhibition byproduct (see text).

to be the first-order in [catalyst]. Overall, the empirical rate law can then be expressed as in eq 11 and is identical to that for organolanthanide-catalyzed aminoalkene,[8j] aminoalkyne,[10c] and aminoallene[11b] hydroamination/cyclization.

$$\nu = k[\text{substrate}]^0[\text{Ln}]^1 \qquad (11)$$

Variable temperature kinetic measurements were also carried out for the **1** → **2a/b** cyclization mediated by Cp′$_2$LaCH(TMS)$_2$ and indicate the reaction to be zero-order in substrate concentration over a greater than 30 °C temperature range (Figure 7A). Standard Arrhenius and Eyring kinetic analyses[40] (Figure 7B) afford the activation parameters E_a = 11.0 (0.4) kcal/mol, $\Delta H^{\ddagger}$ = 10.4 (0.4) kcal/mol, and $\Delta S^{\ddagger}$ = −32.7 (1.2) cal/K mol.[41]

A.

$y = 52.182x - 90.097$
$R^2 = 0.9984$

(x-axis: [Catalyst] mM; y-axis: Rate (mM/h))

B.

$y = 1.2215x + 3.179$
$R^2 = 0.9988$

(x-axis: ln([cat]); y-axis: ln(rate))

Figure 6. (A) Determination of reaction order in lanthanide concentration for the hydroamination/cyclization of (4E,6)-heptadien-1-amine (**1**) using the precatalyst Cp′$_2$LaCH(TMS)$_2$ in benzene-d_6 at 25 °C. (B) van't Hoff plot for the hydroamination/cyclization of (4E,6)-heptadien-1-amine (**1**) using the precatalyst Cp′$_2$LaCH(TMS)$_2$ in benzene-d_6 at 25 °C. The lines are least-squares fits to the data points.

Discussion

Substituent, Metal, and Ancillary Ligand Effects on Catalytic Activity. Rates of aminodiene cyclization are far more rapid than those for internal alkene hydroamination[8c] and are comparable to or even faster than those for terminal alkene hydroamination[8j] (Table 2). This ordering can be viewed as a substituent group effect on the rate of aminoalkene hydroamination, and N_t increases in the order Me ≪ H < vinyl for Cp′$_2$-La− or Me$_2$Si(OHF)(CpR*)Sm− catalyzed reactions. Furthermore, N_t also varies with terminal dienyl group substituent in the order of Me ≪ H < Ph (Cp′$_2$Sm− catalyst, Table 1, entries 2, 14, 16) or Me ≪ Ph < H (Cp′$_2$La− catalyst, Table 1, entries 1, 13, 15) for cyclization **1** → **2**. These two substituent effects qualitatively confirm the proposed transition state electronic demand model (**C**).[42] Similar substituent effects were previously proposed for aminoalkyne cyclization[10c] and explained by assuming an analogous structure (**D**).

D
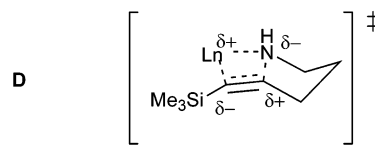
Metal and ancillary ligation effects on aminodiene hydroamination qualitatively parallel those for aminoalkene hydroami-

(40) Benson, S. W. *Thermochemical Kinetics*, 2nd ed.; Wiley: New York, 1986; pp 8−10.
(41) Parameters in parentheses represent 3σ values derived from the least-squares fit.
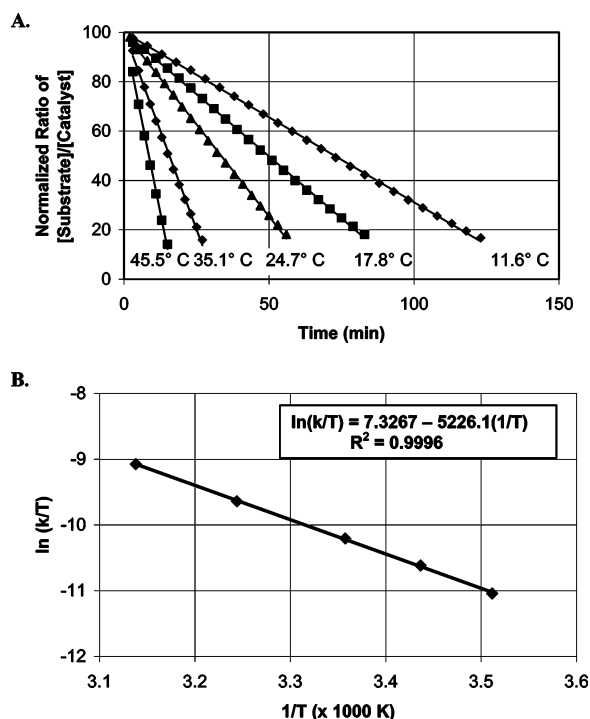
Figure 7. (A) Normalized ratio of substrate to lanthanide as a function of time and temperature for the hydroamination/cyclization of (4*E*,6)-heptadien-1-amine (**1**) using the precatalyst Cp′$_2$LaCH(TMS)$_2$ in benzene-d_6. (B) Eyring plot for the hydroamination/cyclization of (4*E*,6)-heptadien-1-amine (**1**) using the precatalyst Cp′$_2$LaCH(TMS)$_2$ in benzene-d_6. The lines are least-squares fits to the data points.

nation/cyclization.[8j] N_t increases with larger lanthanide ionic radii and *approximately* with more open ligation. However, note that N_t varies much more dramatically with subtle changes in metal ionic radius than in other catalytic systems. For example, aminoalkene hydroamination exhibits a change of $\sim 10^3 \times$ that from La$^{3+} \rightarrow$ Lu^{3+} for the cyclization of 2,2-dimethyl-4-penten-1-amine (eq 12), whereas the present catalytic system exhibits $> 10^3 \times$ change from La$^{3+} \rightarrow$ Y^{3+} (Table 1, entries 1−3), arguing for a more sterically demanding transition state in the turnover-limiting step. To judge relative coordinative openness
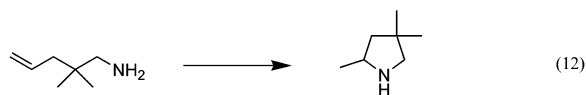
in closely related metallocene ligand structures, the centroid-metal-centroid/amido angles are often compared. Thus, chelating ancillary ligands such as Me$_2$SiCp″(CpR*) ($\angle = 121°$ for SmN-(TMS)$_2$),[9b] Me$_2$Si(OHF)(CpR*) ($\angle = 122°$ for YN(TMS)$_2$),[9a] Me$_2$SiCp″$_2$ ($\angle = 122°$ for NdCH(TMS)$_2$),[32] and Me$_2$SiCp″-*t*BuN) ($\angle = 95°$ for SmN(TMS)$_2$)[8g] are more open than Cp′$_2$ ($\angle = 134°$ for NdCH(TMS)$_2$).[16c] For cyclization **1** → **2**, N_t increases $\sim 10^2 \times$ that from Cp′$_2$ to the Me$_2$SiCp″(CpR*) ancillary ligand. However, the relative reactivity order between the Me$_2$Si(OHF)(CpR*) and CGC ligand frameworks varies with substrate, and sometimes Me$_2$Si(OHF)(CpR*) exhibits slightly greater N_t values, although CGC ligation is generally considered to be more open. Since the CGCSm− catalyst tends to exhibit

(42) Methyl substitution leads to a destabilization of the proposed transition state **C** relative to R = H or Ph; however, a reversed H versus Ph substituent effect for two different lanthanide catalysts appears to imply competing steric effects as well.
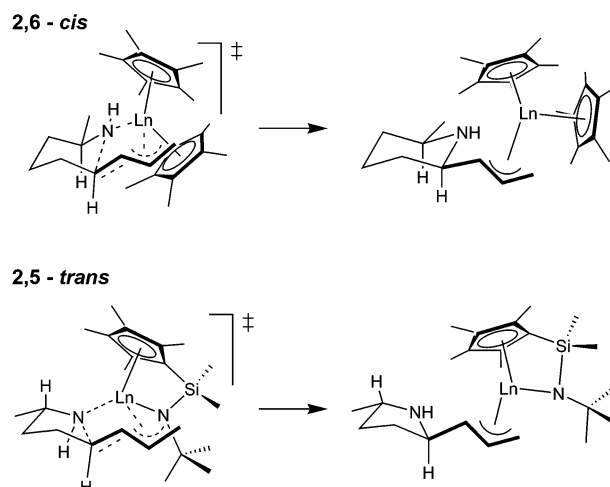
Figure 8. Plausible transition states for diastereoselective aminodiene hydroamination/cyclization.

slightly different kinetic behavior (more pronounced competitive product inhibition) in aminodiene cyclization, factors other than steric (e.g., a greater number of coordinated amine ligands arrayed about the metal center, depressing otherwise more rapid reaction rates) may also contribute to the activity of CGCSm− complexes.

Overall, conjugated aminodiene cyclizations appear to take advantage of electronic effects (stabilization of electronic demands) in the insertive transition state, leading to rate enhancement. However, the turnover-limiting olefin insertion step is even more sterically demanding than in aminoalkene cyclizations.

Diastereo- and Enantioselectivity of Aminodiene Hydroamination/Cyclization. Good to excellent diastereoselectivities are observed in 2,5-*trans*-disubstituted pyrrolidine and 2,6-*cis*-disubstituted piperidine cyclizations. The high diastereoselectivities can be rationalized by assuming chairlike transition states in which methyl and diene units occupy thermodynamically more stable equatorial positions (minimal 1,3-diaxial interactions; Figure 8). In addition, the depicted stereoselection model does not exhibit any unfavorable nonbonding interactions between substrate and catalyst, which also can affect the stereochemical outcome. Therefore, this model accounts well for the observed diastereoselectivity.

The steric demands of the putative η^3-allyl intermediate greatly influence the stereochemical outcome of enantioselective aminodiene hydroamination/cyclization. Compared with homologous aminoalkene cyclization (Tables 4 and 5),[9] enantioselectivity *decreases* ca. 20−40% for five-membered ring formation (Table 4, entries 1−4 vs Table 5 entries 1−4), whereas it *increases* substantially, from 10% to 63%, for six-membered ring formation (Table 4, entries 5−13 vs Table 5, entry 5). Interestingly, these trends are qualitatively similar to those observed when ancillary ligand steric demands are increased from Me$_2$SiCp″(CpR*)Sm−[9b] to Me$_2$Si(OHF)(CpR*)-Sm−[9a] (Table 5, entries 1 and 6 vs entries 2 and 7). In marked contrast, additional installation of a *gem*-dimethyl group, which was crucial for improved enantioselectivity in piperidine formation for aminoalkene hydroamintion with Me$_2$Si(OHF)(CpR*)-Sm−[9a] (Table 5, entry 6 vs entry 5), actually decreases ee values in aminodiene cyclization (Table 4, entries 14−16). No simple model is available at present to correlate substrate architectural
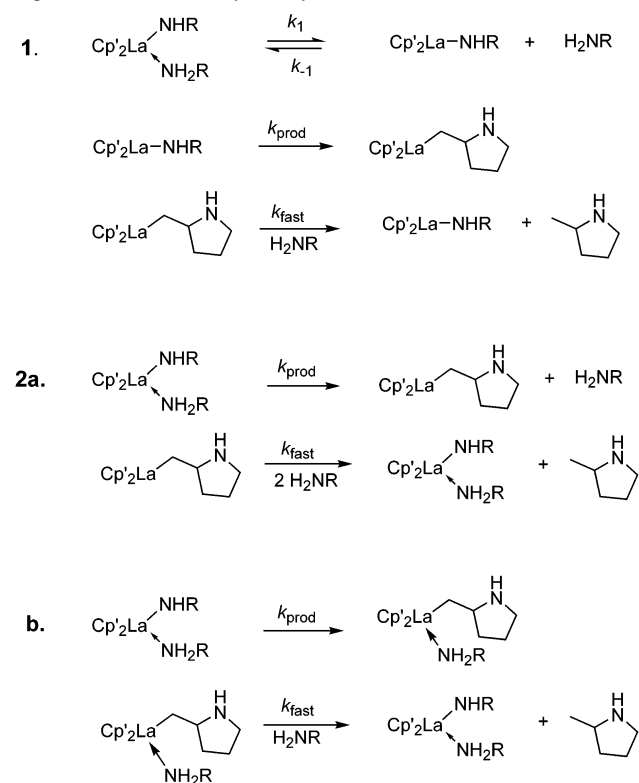
features with enantiomeric excess in these cyclizations. The preliminary studies with chiral Lewis base additives (BINAP[43] and Pfaltz's P,N ligand[44]) reveal that cyclization rates are moderately depressed while ee's remain virtually unchanged, regardless of additive stereochemistry. This can be interpreted as indicating that the additive molecules are likely coordinated to the lanthanide center in the resting state but must dissociate/ be displaced for the sterically demanding insertion process to occur in cyclization **5 → 6**. This scenario will be discussed further in the following section.

Although the enantiomeric excess values presented here still require improvement, the present results constitute another important step forward to general enantioselective hydroamination, potentially one of the most efficient and elegant ways of constructing chiral amine molecules from prochiral unactivated alkenes.

Kinetics and Mechanism of Aminodiene Hydroamination/ Cyclization. The kinetic results for the transformation **1 → 2** catalyzed by Cp′₂LaCH(TMS)₂ indicate zero-order rate dependence on substrate concentration (Figure 2A) and first-order dependence on catalyst concentration (Figure 6), similar to the scenario for intramolecular aminoalkenes,[8j] aminoalkynes,[10c] and aminoallene hydroamination/cyclizations.[11b] This result argues that the turnover-limiting step in the present case involves intramolecular C=C insertion into the Ln–N bond (Scheme 2, step i), followed by rapid protonolysis of the resulting Ln–C bond (Scheme 2, step ii).

However, despite the apparent kinetic similarities, a plot of substrate concentration versus time occasionally departs from the typical linearity (zero-order kinetics) after about the first half-life, affording either depressed rates (seemingly first-order-like kinetic behavior, Figure 3A)[8j,9b,38] or rate acceleration (Figure 3B). Rate depressions are generally associated with CGCSm− catalyzed diene cyclizations at room temperature (Table 1, entries 4 and 8; Table 3, entries 1, 3, 4), whereas rate accelerations are typical of six-membered ring formation mediated by more encumbered Cp′₂Ln− catalysts (Table 1, entries 9−12). Further investigations of the seemingly first-order kinetic behavior using the half-life method in conjunction with the initial rate method reveal that the initial rate is still zero-order in substrate (Figure 4). In addition, a kinetic plot for the second batch cyclization in the presence of the first batch cyclization products clearly indicates more pronounced deviation as well as a depressed reaction rate (Figure 5). These two experiments suggest the observed rate depression is due to competitive inhibition by product. It was previously observed,[8j] and is supported by much independent evidence,[45] that variable numbers of amine molecules are coordinated to the metal center and that these significantly modulate the diastereoselectivity of aminoalkene hydroamination/cyclization as well as influence rates mainly via competition with substrate molecules for the

(43) BINAP = 2,2′-bis(diphenylphosphino)-1,1′-binaphthyl: Noyori, R.; Takaya, H. *Acc. Chem. Res.* **1990**, *23*, 345−350.

(44) Loiseleur, O.; Hayashi, M.; Schmees, N.; Pfaltz, A. *Synthesis* **1997**, 1338−1345.

(45) For example, the X-ray crystal structure of Cp′₂LnNHCH₃(H₂NCH₃) and variable temperature ¹H NMR spectroscopy of Cp′₂LnNHCH₃(H₂NCH₃) were reported.[8j] The formation of amine–amido adducts was proposed to explain hydroamination/cyclization rate laws,[8j] effects of exogeneous bases on reaction rates and diastereoselection in formation of 2,5-dimethylpyrrolidine,[8j] facile intermolecular alkyne insertion competing favorably with intramolecular insertion,[10a] paramagnetic line broadening in the ¹H NMR,[9b] and epimerization of chiral lanthanocene catalysts in the presence of amines.[9a−c] For other related examples, see footnote 38 in ref 10a.

Scheme 4. Mechanistic Scenarios for Organolanthanide-Catalyzed Hydroamination

reaction centers. It has also been observed that the exchange process rapidly permutes not only lanthanide amido and the coordinated amine groups but also coordinated and free amines. These processes are fast on the NMR time scale even at very low temperatures (eq 13).[8j] Since the free-coordinated amine

exchange process should be highly sensitive to the relative coordinating propensity of individual substrate and product amine molecules as well as to the nature of lanthanide metal center as defined by ionic radius and ancillary ligation, the deviation from zero-order substrate kinetic linearity is, in principle, always possible depending upon the particular combination of catalyst, substrate, and product.[46]

On the other hand, rate accelerations or self-inhibition by substrate (Figure 3B) may imply a mechanistic variant. Scheme 4 portrays the two most reasonable mechanistic scenarios selected from those originally considered for Cp′₂Ln− catalyzed hydroamination/cyclization with consideration of turnover-limiting olefin insertion and the possibility of additional bound

(46) Since the free-coordinated amine exchange process in the Cp′₂Ln− metal environment does not involve the secondary heterocyclic cyclization products, it was previously argued that once cyclized, the 2-methyl heterocyles do not effectively compete with substrate for the catalyst center nor function as inhibitors under typical reaction conditions for Cp′₂Ln− catalyzed aminoalkene hydroamination.[8j] However, subsequent in situ ¹H NMR experiments with paramagnetic, more open Me₂SiCp″(CpR*)Ln catalysts (Ln = Nd, Sm) reveal that the product resonances are often broadened after ∼1 half-life, which implies that the product heterocycles are significantly involved in coordination to/amine exchange with the chiral paramagnetic lanthanide amine–amido complexes.[9b]
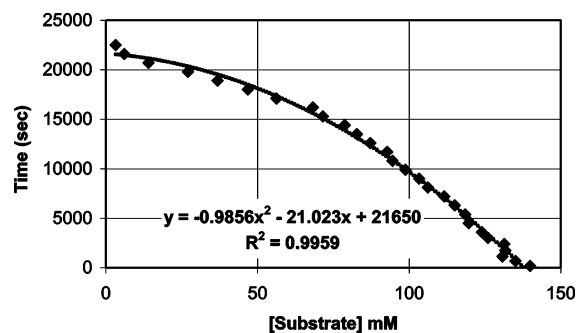
Figure 9. Plot of reaction time versus substrate concentration for the hydroamination/cyclization of (5*E*,7)-octadien-1-amine (**5**) using the precatalyst Cp′$_2$LaCH(TMS)$_2$ in benzene-d_6 at 25 °C.

Table 7. Activation Parameter Comparison for Intramolecular Hydroamination/Cyclization Reactions

Substrate	Catalyst	N_t, h^{-1} (ºC)	$\Delta H^{\ddagger}$, kcal/mol	$\Delta S^{\ddagger}$, eu	$E_a^{\ddagger}$, kcal/mol
⌇⌇⌇NH$_2$	Cp′$_2$La-	40 (25)	10.4 (0.4)	-32.7 (1.2)	10.4 (0.4)
⌇⌇NH$_2$	Cp′$_2$La-	13 (25)	12.7 (1.4)	-27.0 (4.6)	13.4 (1.5)
⌇⌇NH$_2$	Cp′$_2$Sm-	580 (21)	10.7 (8)	-27.4 (6)	-
⌇⌇NH$_2$	Cp′$_2$La-	4 (23)	16.9 (1.3)	-16.5 (4.3)	17.6 (1.4)

amines present at the metal center: (1) amine-free catalyst in equilibrium with an amine adduct (turnover-limiting olefin insertion) and (2) (a) concerted amine displacement from an amine–amido complex in concert with turnover-limiting olefin insertion or (b) permanent amine coordination during turnover-limiting olefin insertion. In scenario 1, the amine adduct is in equilibrium with the amine-free form, the precursor to turnover-limiting olefin insertion. Kinetic analysis using standard steady-state conditions in Cp′$_2$LnNHR[47] yields the rate law of eq 14, in which [S] and [LnN$_2$] are the substrate and amine–amido concentrations, respectively.

$$\text{velocity} = \frac{k_{prod} k_1 [\text{LnN}_2]}{k_{-1}[\text{S}] + k_{prod}} \quad (14)$$

In the previous study of Cp′$_2$Ln– mediated *aminoalkene* hydroamination, this scenario was reasonably excluded on the basis that self-inhibition kinetics are not observed.[8j] In the present study, a kinetic plot of *aminodiene* cyclization **5 → 6a/b** (Figure 3B) appears to follow the steady-state rate expression, and this adherence is further substantiated when a time versus [substrate] plot (Figure 9) is compared with the integrated form of the rate expression, assuming time-independent [LnN$_2$] (eq 15).

$$t = \frac{k_{-1}}{2k_{prod}k_1\,[\text{LnN}_2]}[\text{S}]^2 - \frac{1}{k_1[\text{LnN}_2]}[\text{S}] + \text{constant} \quad (15)$$

Therefore, in the case of piperidine formation mediated by Cp′$_2$Ln– catalysts, additional coordinated amines must dissociate to create a room for sterically demanding diene coordination/insertion. The absence of additional amines in the transition state of these octadienylamine cyclizations is further supported by the aforementioned chiral additive studies, in which enantiomeric access of the piperidine product is not affected by addition of chiral Lewis base.

The present activation parameters for the transformation of **1 → 2a/b** can be compared to the parameters for the hydroamination/cyclization of aminoalkenes,[8j] aminoalkynes,[10c] and aminoallenes[11b] (Table 7). While the aminodiene cyclization exhibits a lower enthalpic barrier than an analogous aminoalkene cylization, the significantly larger magnitude of $\Delta S^{\ddagger}$ (more negative) suggests that the transition state is more highly organized (greater loss of degrees of freedom) than in ami-

noalkene cyclization. Note that the lower $E_a^{\ddagger}$ value (derived from the standard Arrehenius analysis) of aminodiene cyclization versus aminoalkene cyclization provides an explanation for the rate enhancement observed with the dienyl group versus terminal olefin. However, care must be taken in direct comparison of the aminodiene cyclization activation parameters with those for aminoalkyne and aminoallene cyclization, because of the disparities in lanthanide metal ionic radius effects on N_t.[48] Overall, the present results obtained from the kinetic studies (rate law, activation parameters) and from factors affecting cyclization rates (metal ion size, π-ancillary ligand, product ring size, substrate substituent effects) support a mechanistic scenario analogous to the established hydroamination/cylization mechanism (Scheme 2), although the presence and role of coordinating amine ligands in the more sterically sensitive and highly organized transition state may also depend on specific reaction conditions.

Conclusions

The results presented here demonstrate that efficient organolanthanide-catalyzed intramolecular hydroamination/cyclization of amine-tethered 1,2-disubstituted alkenes is achieved using readily accessible conjugated aminodienes. The catalytic reaction proceeds cleanly at 25–60 °C with good rates, high regioselectivities, and with electronic effects leading to significant rate enhancements. Some features of the reaction parallel monosubstituted aminoalkene hydroamination/cyclization, including rate law and effects of lanthanide metal ionic radius and ancillary ligation. Good to excellent diastereoselectivity is obtained in 2,5-*trans*-disubstituted pyrrolidine and 2,6-*cis*-disubstituted piperidine syntheses. Aminodienes offer an enantioselective route to 2-substituted azacycles. The reaction mechanism implicated has both similarities to, and differences from, that defined for aminoalkene hydroamination/cyclization.

(47) (a) Moore, J. W.; Pearson, R. G. *Kinetics and Mechanisms*, 3rd ed.; Wiley: New York, 1981; pp 313–317 and references therein. (b) Segel, I. H. *Enzyme Kinetics*; Wiley: New York, 1975; Chapters 1–3.

(48) N_t increases in the order La^{3+} < Sm^{3+} < Y^{3+} < Lu^{3+} for aminoalkyne cyclizations, whereas N_t increases in the order La^{3+} < Lu^{3+} < Sm^{3+} < Y^{3+} for aminoallene cyclizations.